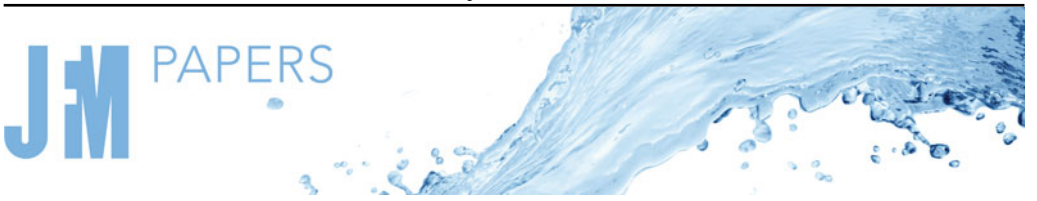
J. Fluid Mech. (2026), *vol.* 1038, A29, doi:10.1017/jfm.2026.11731



Energy dissipation of Oldroyd-B fluids in plane Couette flow

Haoting Grange Chen[1], **Sergei I. Chernyshenko**[1] **and Andrew Wynn**[1]

[1]Department of Aeronautics, Imperial College London, London SW7 2AZ, UK

Corresponding author: Haoting Grange Chen, grange.chen19@imperial.ac.uk

(Received 30 December 2025 UTC; revised 14 May 2026 UTC; accepted 25 May 2026 UTC)

This paper establishes a rigorous upper bound on the infinite-time-averaged energy dissipation rate of Oldroyd-B fluids in plane Couette flow. The bound depends only on system parameters – the Reynolds number, Weissenberg number and viscosity ratio – and applies to all steady and unsteady solutions within a certain region in parameter space. The bound is proven by extending the 'background-flow method' to the case where the system energy is no longer a quadratic functional of the underlying flow fields, and is obtained by using a non-polynomial auxiliary functional related to the free polymeric energy. Within the range of the flow parameters in which the steady solution is known to be globally stable, the dissipation rate of the steady flow is recovered, and in the Newtonian limit the result reduces to the best-known bound for Newtonian Couette flow. Our analysis also identifies a range of parameters for which the total energy of the viscoelastic flow must be bounded, thus ruling out the possibility of energy blow-ups in these situations.

Key words: turbulent flows, non-Newtonian flows

1. Introduction

Flows of non-Newtonian fluids, such as polymer solutions, suspensions and biological fluids, are encountered in many industrial and biological settings, and exhibit markedly different dynamical behaviour from their Newtonian counterparts. It is therefore of interest to quantify how key flow statistics, such as the time-averaged energy dissipation rate, scale with the system parameters. The established approach for proving bounds on energy dissipation rate in Newtonian fluid mechanics is the 'background-flow method' (Doering & Constantin 1992, 1994, 1995), which extends classical stability analysis to give information about a flow in its unsteady or turbulent regimes. Unfortunately, despite

© The Author(s), 2026. Published by Cambridge University Press. This is an Open Access article, distributed under the terms of the Creative Commons Attribution licence (https://creativecommons.org/licenses/by/4.0/), which permits unrestricted re-use, distribution and reproduction, provided the original article is properly cited.

https://doi.org/10.1017/jfm.2026.11731 Published online by Cambridge University Press

the background method's success in proving dissipation estimates for Newtonian channel flows, it is not obvious how to extend this analysis to the viscoelastic setting due to the non-polynomial nature of the total energy. We overcome this difficulty by using the auxiliary-functional method (Chernyshenko *et al.* 2014), which allows analysis of general functionals of the underlying flow, to prove rigorous bounds on dissipation for Oldroyd-B fluids in Couette flow. To our knowledge, this is the first use of a non-polynomial auxiliary functional for proving dissipation rate bounds in fluid mechanics.

The distinctive behaviour of viscoelastic fluids partly stems from the fact that, in addition to energy dissipation by viscous effects, energy may be both stored and dissipated through polymer stretching and relaxation. These elastic effects support turbulence-like regimes that have no direct counterparts in Newtonian fluids. It has been shown that, across geometries, dilute polymer solutions can reduce drag (Metzner & Park 1964; Jones & Maddock 1966), increase pressure losses (Metzner & White 1965) and elevate dissipation (Rothstein & McKinley 2001). Elasticity not only modifies dissipation, but can also by itself drive and reorganise flows, even when inertia is negligible. In Taylor–Couette flow, dilute polymer solutions exhibit a purely elastic instability at negligible inertia driven by normal stresses (Larson, Shaqfeh & Muller 1990; Shaqfeh 1996), and even small polymer additions shift the stability threshold into elasticity-dominated regimes (Groisman & Steinberg 1996, 1998). At higher forcing in similar low-inertia settings, the flow enters a regime known as elastic turbulence, sustained by elastic stresses rather than inertia (Groisman & Steinberg 2000). At moderate Reynolds numbers, polymer triggers elasto-inertial turbulence at Reynolds numbers well below the Newtonian threshold (Samanta *et al.* 2013), while at high Reynolds number drag reduction approaches the maximum-drag-reduction asymptote (Virk 1975). Collectively, these results show that polymer stresses both reorganise the flow and sustain turbulence-like dynamics. Consequently, any energy analysis must account for storage and relaxation in the polymer as well as viscous effects (Shaqfeh 1996; Rothstein & McKinley 2001).

The increased complexity of viscoelastic flows is also demonstrated by the fact that numerical simulations are prone to difficulties even in relatively benign parameter regions. The 'high Weissenberg number problem' is a well-known phenomenon in which computations lose convergence beyond a critical Weissenberg number (Keunings 1986). For example, even though plane Couette flow of upper-convected Maxwell and Oldroyd-B fluids is linearly stable in the inertialess limit (Renardy 1992, 1993), numerical simulations can still display spurious instabilities (Keiller 1992). Energy-consistent discretisations (Lozinski & Owens 2003), recognition that Oldroyd-B fluids can develop near-singular stress structures due to the absence of polymeric diffusion (Thomases & Shelley 2007), and symmetric positive-definiteness preserving conformation-tensor formulations (Balci *et al.* 2011) mitigate aspects of the issues, but do not eliminate them. Loss of numerical stability is observed in non-planar geometries at Weissenberg numbers of order one (Lee, Hwang & Cho 2021). Consequently, robust numerics at even modest Weissenberg numbers remain open in general (Renardy & Thomases 2021). This motivates the desire to obtain relevant rigorous results such as theorems on bounds on the time-averaged energy dissipation rate, or on the boundedness of instantaneous energy values.

In this paper, we study how large energy dissipation can be for Oldroyd-B fluids in plane Couette flow. A recent step towards this direction is the work by Binns & Wynn (2024), who, by constructing a non-polynomial Lyapunov functional, established global nonlinear stability for Oldroyd-B fluids in plane Couette flow within a certain range of flow parameters. However, outside this region, this result does not provide information about the energy dissipation rate, notably for higher Reynolds numbers. We address this

https://doi.org/10.1017/jfm.2026.11731 Published online by Cambridge University Press

gap by deriving rigorous upper bounds on the infinite-time-averaged energy dissipation rate across a broader region in parameter space.

In pursuit of dissipation bounds for viscoelastic fluids, it is natural to first inspect similar results for Newtonian fluids. Variational methods have been successful in bounding transport and dissipation in Newtonian plane Couette flow (Hopf 1950; Howard 1963; Busse 1978). A major conceptual advancement came with the background-flow method of Doering & Constantin (1992, 1994, 1995), within which tighter bounds were also obtained numerically (Nicodemus *et al.* 1997*a*,*b*, 1998; Plasting & Kerswell 2003). We now extend the background-flow method for Newtonian fluids to the more complex viscoelastic fluids, by utilising a non-polynomial auxiliary functional and choosing a polymer background profile.

We will prove for any Weissenberg number $0 < Wi < 1$ and viscosity ratio $0 < \beta < 1$, that if the Reynolds number satisfies $0 < Re < 4\sqrt{2}\beta(1 + Wi^{-1})$ then the infinite-time-averaged energy dissipation rate is bounded above

$$\overline{\mathcal{E}} \leq \left(\frac{1}{1 - Wi}\right)\left(\frac{1}{8\sqrt{2}} + \frac{(\sqrt{2} - 1)(1 - \beta)}{2\beta(1 + Wi)}\right)\max\left\{1, \frac{8\sqrt{2}\beta}{Re}\right\}. \tag{1.1}$$

This estimate holds for all solutions to the system, and coincides with the bound on Newtonian dissipation presented by Doering & Constantin (1992) in the Newtonian limit $\beta \to 1$, $Wi \to 0$ for large Reynolds numbers. Although the results are restricted to small Weissenberg numbers, they apply at arbitrarily high Reynolds numbers where one would certainly expect turbulence. We refer the reader to § 4.3 for the origin of the above parameter restriction, which arises from the compatibility conditions imposed on the auxiliary-functional parameters. We also discuss possible ways to relax this restriction, for example by adopting a constitutive model that regularises the polymer conformation tensor, such as the Oldroyd-B model with polymeric diffusion or the finitely extensible nonlinear elastic-Peterlin (FENE-P) model.

The paper is organised as follows: we first examine the global stability result by Binns & Wynn (2024), then extend the background-flow method such that it applies to viscoelastic settings – where the natural energy functional is not quadratic – by employing the auxiliary-functional approach. This enables us to derive a rigorous upper bound on the infinite-time-averaged energy dissipation and, at the same time, prove energy boundedness of the viscoelastic flow for a certain range of parameter values.

2. Oldroyd-B fluids in plane Couette flow

Consider an incompressible viscoelastic fluid flow with velocity $\boldsymbol{u} = u_x\boldsymbol{e}_x + u_y\boldsymbol{e}_y + u_z\boldsymbol{e}_z$ between two parallel plates at $y = 0$ and $y = \ell$. The bottom plate is stationary and the top plate is travelling at velocity U in the $\boldsymbol{e}_x$ direction. Periodic boundary conditions are imposed on the $\boldsymbol{e}_x$ and $\boldsymbol{e}_z$ directions and no-slip conditions are assumed at the upper and lower boundaries.

In the Oldroyd-B model, polymers dissolved in the fluid solvent are modelled as dumbbells which are advected, stretched and rotated by the flow. The stress tensor $\boldsymbol{T}$ in the momentum equation

$$\rho\left[\frac{\partial \boldsymbol{u}}{\partial t} + (\boldsymbol{u}\cdot\nabla)\boldsymbol{u}\right] = \nabla\cdot\boldsymbol{T} - \nabla p \tag{2.1}$$

consists of both contributions from the solvent and polymer via

$$\boldsymbol{T} = \boldsymbol{T}_p + \eta_s\left[\nabla\boldsymbol{u} + (\nabla\boldsymbol{u})^{\top}\right], \tag{2.2}$$

https://doi.org/10.1017/jfm.2026.11731 Published online by Cambridge University Press

where ρ is the density, η_s is the solvent viscosity, p is the pressure and $\boldsymbol{T}_p$ is the polymeric contribution to the stress tensor. This is assumed to satisfy the upper-convected Maxwell equation

$$\lambda\left[\frac{\partial \boldsymbol{T}_p}{\partial t}+\boldsymbol{u}\cdot\nabla\boldsymbol{T}_p-\boldsymbol{T}_p\cdot\nabla\boldsymbol{u}-(\nabla\boldsymbol{u})^{\top}\cdot\boldsymbol{T}_p\right]+\boldsymbol{T}_p=\eta_p\left[\nabla\boldsymbol{u}+(\nabla\boldsymbol{u})^{\top}\right], \tag{2.3}$$

where η_p is the polymer viscosity and λ is the characteristic relaxation time scale of the dissolved polymers.

The standard non-dimensionalisation of the system is performed using ℓ as a characteristic length scale, U as a velocity scale, ℓ/U as the associated time scale and by introducing the polymer conformation tensor

$$\boldsymbol{c}=\frac{\lambda}{\eta_p}\boldsymbol{T}_p+\boldsymbol{I}, \tag{2.4}$$

where $\boldsymbol{I}$ is the identity matrix. Denoting the resulting non-dimensional quantities again by $\boldsymbol{u}$ and p, the non-dimensional system reads

$$\frac{\partial \boldsymbol{u}}{\partial t}+(\boldsymbol{u}\cdot\nabla)\boldsymbol{u}+\nabla p=\frac{\beta}{Re}\nabla^2\boldsymbol{u}+\frac{1-\beta}{ReWi}\nabla\cdot\boldsymbol{c}, \tag{2.5a}$$

$$\nabla\cdot\boldsymbol{u}=0, \tag{2.5b}$$

$$\frac{\partial \boldsymbol{c}}{\partial t}+(\boldsymbol{u}\cdot\nabla)\boldsymbol{c}=\boldsymbol{c}\cdot\nabla\boldsymbol{u}+(\nabla\boldsymbol{u})^{\top}\cdot\boldsymbol{c}+\frac{1}{Wi}(\boldsymbol{I}-\boldsymbol{c}), \tag{2.5c}$$

on the domain $\Omega=[0,\,\Gamma_x]\times[0,\,1]\times[0,\,\Gamma_z]$ with boundary conditions

$$\begin{aligned}&\boldsymbol{u}(x,\,y,\,z)=\boldsymbol{u}(x+\Gamma_x,\,y,\,z), \quad &&\boldsymbol{u}(x,\,y,\,z)=\boldsymbol{u}(x,\,y,\,z+\Gamma_z),\\ &\boldsymbol{c}(x,\,y,\,z)=\boldsymbol{c}(x+\Gamma_x,\,y,\,z), \quad &&\boldsymbol{c}(x,\,y,\,z)=\boldsymbol{c}(x,\,y,\,z+\Gamma_z),\\ &\boldsymbol{u}(x,\,0,\,z)=0, &&\boldsymbol{u}(x,\,1,\,z)=\boldsymbol{e}_x.\end{aligned} \tag{2.6}$$

The system's behaviour is governed by three non-dimensional parameters

$$Re=\frac{\rho U\ell}{\eta}, \qquad \beta=\frac{\eta_s}{\eta}, \qquad Wi=\frac{U\lambda}{\ell}, \tag{2.7}$$

where the Reynolds number Re is defined in terms of the total viscosity $\eta=\eta_s+\eta_p$, the Weissenberg number Wi is the ratio between the characteristic time scale of the polymer to that of the fluid and β is the ratio of solvent viscosity to total viscosity.

No boundary conditions are needed for $\boldsymbol{c}$ at the walls. The constitutive equation (2.5c) is first order in space: the only spatial derivative of $\boldsymbol{c}$ appears through the transport term $\boldsymbol{u}\cdot\nabla\boldsymbol{c}$. Since the velocity field satisfies the no-penetration condition $\boldsymbol{u}\cdot\boldsymbol{n}=0$ at the walls, there is no inflow boundary through which information on the conformation tensor must be supplied. However, it is useful to note that $\boldsymbol{c}$ can be viewed as the covariance matrix of the end-to-end point vectors of the polymer dumbbells. As a result, it is natural that $\boldsymbol{c}$ is symmetric and positive definite, which we write in the standard notation $\boldsymbol{c}=\boldsymbol{c}^{\top}\succ 0$. It is well known that if initially

$$\boldsymbol{c}(\boldsymbol{x},\,0)=\boldsymbol{c}^{\top}(\boldsymbol{x},\,0)\succ 0, \qquad \boldsymbol{x}\in\Omega, \tag{2.8}$$

then this property holds for solutions of (2.5c) for all subsequent times. Therefore, any such solution of the Oldroyd-B equations (2.5a–c) at each time instant belongs to the set $\mathcal{S}$ (Binns & Wynn 2024), defined as

$$\mathcal{S}:=\left\{(\boldsymbol{u},\,\boldsymbol{c}):\ \begin{array}{c}\boldsymbol{u}\text{ satisfies the boundary conditions (2.6)}\\ \nabla\cdot\boldsymbol{u}=0\text{ and }\boldsymbol{c}=\boldsymbol{c}^{\top}\succ 0\end{array}\right\}. \tag{2.9}$$

https://doi.org/10.1017/jfm.2026.11731 Published online by Cambridge University Press

2.1. *Energy dissipation*

Our aim is to understand how the energy dissipation rate of Oldroyd-B fluids in plane Couette flow depends on the three governing parameters (β, Re, Wi). We follow the widely accepted formulation of total energy of Oldroyd-B fluids (Doering, Eckhardt & Schumacher 2006; Hu & Lelièvre 2007; Boyaval, Lelièvre & Mangoubi 2009; Lukáčová−Medvid'ová *et al.* 2016)

$$E := \frac{1}{2}\,\|\boldsymbol{u}\|^2 + \frac{1-\beta}{2Re\,Wi}\int_\Omega \operatorname{tr}(\boldsymbol{c}-\boldsymbol{I}) - \log\det\boldsymbol{c}\,\mathrm{d}V, \tag{2.10}$$

which can be interpreted as the sum of the fluid's kinetic energy and the potential energy stored in the polymers. This is the standard thermodynamically consistent free-energy formulation for the Oldroyd-B model (Hu & Lelièvre 2007). The important property for the present analysis is that differentiating (2.10) along trajectories yields the balance (2.13), with a non-negative polymer dissipation density $\operatorname{tr}(\boldsymbol{c}+\boldsymbol{c}^{-1}-2\boldsymbol{I})$. Thus the analysis relies on the free-energy/dissipation structure of the constitutive model, rather than on the particular formulation of the polymer energy. Other constitutive models may have different free energies, but the same strategy is expected to apply whenever an analogous energy balance with non-negative polymer dissipation is available.

Here, and in what follows, we use the following notation for L^2 inner product and norm:

$$\langle \boldsymbol{u}, \boldsymbol{v}\rangle = \int_\Omega \boldsymbol{u}\cdot\boldsymbol{v}\,\mathrm{d}V, \qquad\qquad \|\boldsymbol{u}\|^2 = \langle \boldsymbol{u}, \boldsymbol{u}\rangle\,. \tag{2.11}$$

Along trajectories of the flow (2.5), it follows from the Jacobi formula $(\partial/\partial t)\log\det\boldsymbol{c} = \operatorname{tr}(\boldsymbol{c}^{-1}(\partial\boldsymbol{c}/\partial t))$ that

$$\frac{\mathrm{d}E}{\mathrm{d}t} = \int_\Omega \boldsymbol{u}\cdot\frac{\partial\boldsymbol{u}}{\partial t}\,\mathrm{d}V + \frac{1-\beta}{2Re\,Wi}\int_\Omega \operatorname{tr}\left[\left(\boldsymbol{I}-\boldsymbol{c}^{-1}\right)\frac{\partial\boldsymbol{c}}{\partial t}\right]\mathrm{d}V. \tag{2.12}$$

Substituting (2.5*a*) and (2.5*c*) into the above equation, using incompressibility (2.5*b*) and boundary conditions (2.6) gives the energy equation

$$\begin{aligned}\frac{\mathrm{d}E}{\mathrm{d}t} = &-\frac{\beta}{Re}\,\|\nabla\boldsymbol{u}\|^2 - \frac{1-\beta}{2Re\,Wi^2}\int_\Omega \operatorname{tr}\big(\boldsymbol{c}+\boldsymbol{c}^{-1}-2\boldsymbol{I}\big)\,\mathrm{d}V\\ &+\frac{\beta}{Re}\int_{y=1}\frac{\partial u_x}{\partial y}\,\mathrm{d}A + \frac{1-\beta}{Re\,Wi}\int_{y=1} c_{xy}\,\mathrm{d}A.\end{aligned} \tag{2.13}$$

The first two terms in (2.13) are necessarily negative, while the final two boundary integrals are associated with the power required to enforce the boundary conditions on the upper surface. We therefore interpret the first two terms as the energy dissipation rate

$$\mathcal{E} = \frac{\beta}{Re}\,\|\nabla\boldsymbol{u}\|^2 + \frac{1-\beta}{2Re\,Wi^2}\int_\Omega \operatorname{tr}\big(\boldsymbol{c}+\boldsymbol{c}^{-1}-2\boldsymbol{I}\big)\,\mathrm{d}V \tag{2.14}$$

and the last two as production

$$\mathcal{P} = \frac{\beta}{Re}\int_{y=1}\frac{\partial u_x}{\partial y}\,\mathrm{d}A + \frac{1-\beta}{Re\,Wi}\int_{y=1} c_{xy}\,\mathrm{d}A. \tag{2.15}$$

If we assume that $E(t)$ is uniformly bounded along trajectories of the system then, taking the time average of (2.13) gives

$$\overline{\mathcal{E}} = \overline{\mathcal{P}}, \tag{2.16}$$

https://doi.org/10.1017/jfm.2026.11731 Published online by Cambridge University Press

where $\overline{\mathcal{E}} = \limsup_{T\to\infty}(1/T)\int_0^T \mathcal{E}(\boldsymbol{u}(t), \boldsymbol{c}(t))\,\mathrm{d}t$.

The aim of this paper is to prove – for a range of parameter values (β, Re, Wi) – rigorous upper bounds on the magnitude of the averaged energy dissipation rate $\overline{\mathcal{E}}$ which must hold for any possible realisation of the flow. To do this, we will use the auxiliary-functional method (Chernyshenko *et al.* 2014).

3. The auxiliary-functional method

The key step in proving the energy balance (2.16) was to observe that

$$\overline{\frac{\mathrm{d}}{\mathrm{d}t}E[\boldsymbol{u}(t), \boldsymbol{c}(t)]} = 0 \tag{3.1}$$

holds if energy is bounded along trajectories of the system. The auxiliary-functional method uses a similar observation but with energy replaced by an arbitrary 'auxiliary' functional in order to prove bounds for time averages.

In particular, for any functional $V : (\boldsymbol{u}, \boldsymbol{c}) \to \mathbb{R}$, let $\mathcal{L}_V$ be the functional representing the Lie derivative of V, meaning that

$$\frac{\mathrm{d}}{\mathrm{d}t}V[\boldsymbol{u}(t), \boldsymbol{c}(t)] = \mathcal{L}_V[\boldsymbol{u}(t), \boldsymbol{c}(t)] \tag{3.2}$$

for any solution $(\boldsymbol{u}(t), \boldsymbol{c}(t))$ of (2.5*a–c*). If $V[\boldsymbol{u}(t), \boldsymbol{c}(t)]$ is bounded along trajectories of the system, it then follows that

$$\overline{\mathcal{L}_V[\boldsymbol{u}(t), \boldsymbol{c}(t)]} = 0. \tag{3.3}$$

As an example, the energy equation (2.13) implies the functional equality $\mathcal{L}_E = -\mathcal{E} + \mathcal{P}$, and its time average along trajectories of the system gives (2.16).

This idea can be generalised since (3.3) implies that every acceptable V satisfies the equality

$$\overline{\mathcal{E}[\boldsymbol{u}(t), \boldsymbol{c}(t)]} = \overline{(\mathcal{E} + \mathcal{L}_V)[\boldsymbol{u}(t), \boldsymbol{c}(t)]} \tag{3.4}$$

along trajectories of the system. This gives many different ways to express the time average of energy dissipation. To exploit them, we search for a functional V which satisfies an upper bound of the form

$$(\mathcal{E} + \mathcal{L}_V)\,[\boldsymbol{u}, \boldsymbol{c}] \le \kappa \qquad \forall\,(\boldsymbol{u}, \boldsymbol{c}) \in \mathcal{S}, \tag{3.5}$$

where $\kappa \in \mathbb{R}$ is a constant and $\mathcal{S}$ is the admissible, forward-invariant set (2.9). Since we know all solutions to the Oldroyd-B model belong to $\mathcal{S}$ if they do so initially, it follows from time-averaging (3.5) that $\overline{\mathcal{E}} \le \kappa$ for any such trajectory. This observation is a special case of the following weaker, but sufficient for our case, version of the general result (Chernyshenko *et al.* 2014; Chernyshenko 2022, Theorem 2.2).

LEMMA 1. *Consider a dynamical system whose state $q(t)$ remains in a set $\mathcal{A}$ for all $t \ge 0$. Let $\mathcal{L}_F[q]$ denote the Lie derivative of a functional $F[q]$ with respect to the system, such that $(\mathrm{d}/\mathrm{d}t)F[q(t)] = \mathcal{L}_F[q(t)]$ along trajectories of the system. Let $X[q]$ be a functional of interest.*
If there exists a functional $V[q]$ and a constant κ such that:

(i) $V[q(t)]$ is bounded along all trajectories with $(q(t))_{t\ge0} \subseteq \mathcal{A}$;
(ii) $(X + \mathcal{L}_V)[q] \le \kappa$ for all $q \in \mathcal{A}$;

then for every such trajectory the infinite-time-averaged inequality $\overline{X} \le \kappa$ holds.

https://doi.org/10.1017/jfm.2026.11731 Published online by Cambridge University Press

The key advantage of using the auxiliary-functional method is that inequality (3.5) can be checked without solving the partial differential equations. Given a candidate functional V, one only needs to verify that $\mathcal{E} + \mathcal{L}_V$ is bounded on the admissible set $\mathcal{S}$. Since $\mathcal{S}$ is relatively simple, this can be easier than directly computing the average dissipation $\overline{\mathcal{E}}$. While auxiliary functionals provide arbitrarily sharp bounds on time averages (Tobasco, Goluskin & Doering 2018; Rosa & Temam 2020), this might require constructing more 'intricate' auxiliary functionals V, which, essentially, seek to mathematically extract the correct physics.

To highlight the difficulties involved, suppose we take $V = E$. Then (3.5) becomes

$$(\mathcal{E} + \mathcal{L}_V)[\boldsymbol{u}, \boldsymbol{c}] = \mathcal{P}[\boldsymbol{u}, \boldsymbol{c}] = \frac{\beta}{Re}\int_{y=1} \frac{\partial u_x}{\partial y}\,\mathrm{d}A + \frac{1-\beta}{Re\,Wi}\int_{y=1} c_{xy}\,\mathrm{d}A. \tag{3.6}$$

However, since flow and polymer fields in $\mathcal{S}$ can become arbitrarily large, there is no constant κ for which the inequality (3.5) can hold in this case. That is, while we can assert that $\overline{\mathcal{E}} = \overline{\mathcal{P}}$, we cannot rigorously say anything about the size of either of these quantities.

The classical way to obtain bounds for time averages is the background-flow method (Doering & Constantin 1992, 1994, 1995). This is a special case of the auxiliary-functional method in which one seeks an auxiliary functional in the form of the energy of flow perturbations from a suitably selected 'background flow', multiplied by a constant $\Lambda > 0$ called a 'balancing parameter'. The background-flow method has found wide application for Newtonian fluids ($\beta = 1$, $Re \neq 0$, $Wi = 0$) and, in this setting, corresponds to studying auxiliary functionals V of the form

$$V[\boldsymbol{u}] = \text{Const}\ \|\boldsymbol{u} - \boldsymbol{b}\|^2\,, \tag{3.7}$$

where $\boldsymbol{b}$ is the background flow which can be chosen to shape V.

For Newtonian Couette flow, a typical choice is to take $\boldsymbol{b} = b(y)\,\boldsymbol{e}_x$ as a pure shear profile. At sufficiently low Reynolds numbers, the choice of $\boldsymbol{b}$ which gives the best bound (i.e. the lowest possible κ in (3.5)) is the steady solution and the corresponding bound is $\kappa = \mathcal{E}_{steady} = 1/Re$. For higher Reynolds numbers, the optimal choice of $\boldsymbol{b}$ is known to develop a boundary-layer-like structure indicated in figure 1 (Doering & Constantin 1992), and the exact optimal shape of $b(y)$ must be determined numerically (Plasting & Kerswell 2003). (Also see Rajkotia-Zaheer & Goluskin 2026 for more rigorous justification of these numerical results.) Via (3.5), this optimisation gives an Re-dependent upper bound $\overline{\mathcal{E}} \leq \kappa(Re)$. At low Reynolds numbers this bound coincides with the laminar dissipation $1/Re$, while at high Reynolds numbers the best available background-method bounds approach an $\mathcal{O}(1)$ constant. In this sense, the method captures the transition from the steady Couette scaling to a Reynolds-number-independent upper bound relevant to turbulent Couette flow.

To date, neither the auxiliary nor the background-flow method has been applied to viscoelastic flows. In Newtonian flow, a quadratic kinetic-energy functional is natural since the advection term does not contribute to the energy balance: $\langle \boldsymbol{u}, \boldsymbol{u}\cdot\nabla\boldsymbol{u}\rangle = 0$. The same cancellation remains available for the velocity field in the Oldroyd-B equations, which is why the velocity-dependent part of the auxiliary functional below remains quadratic. The additional difficulty is that the constitutive equation contains the stretching terms $\boldsymbol{c}\cdot\nabla\boldsymbol{u} + (\nabla\boldsymbol{u})^\top\cdot\boldsymbol{c}$. The trace/logarithmic structure of the Oldroyd-B free energy is what gives the cancellation underlying the energy equation (2.13): the terms produced by polymer stretching cancel with a polymer stress-work term in the kinetic-energy balance, while polymer relaxation gives a sign-definite dissipation. As a result, the natural polymer-dependent part of the auxiliary functional is non-polynomial in $\boldsymbol{c}$. In the Newtonian

https://doi.org/10.1017/jfm.2026.11731 Published online by Cambridge University Press

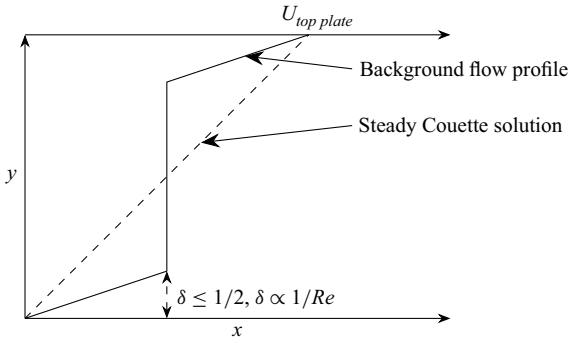


Figure 1. Steady Couette solution and an example background-flow profile. Here δ denotes the boundary-layer thickness of the background-flow profile.

case, the search for the best V can be viewed as searching over auxiliary functionals obtained by adding to the quadratic energy a term that is linear in the state, together with a constant, since the associated background-flow functional in (3.7) can be written as $V[\boldsymbol{u}] = \text{const}\,(\|\boldsymbol{u}\|^2 - 2\langle \boldsymbol{b}, \boldsymbol{u}\rangle + \|\boldsymbol{b}\|^2)$. Polymeric perturbation energies derived from (2.10) are non-polynomial, and this significantly complicates the subsequent analysis.

4. Bounds on energy dissipation for Oldroyd-B fluids in plane Couette flow

Throughout, we will use the following decomposition of the fluid and polymer fields

$$\boldsymbol{u} = \boldsymbol{b} + \boldsymbol{v}, \qquad \boldsymbol{c} = \boldsymbol{c}_b + \boldsymbol{d}, \tag{4.1}$$

where $\boldsymbol{b}$ and $\boldsymbol{c}_b$ are independent of time, satisfy the boundary conditions (2.6) and $\nabla \cdot \boldsymbol{b} = 0$. These choices imply that the velocity perturbation $\boldsymbol{v}$ satisfies homogeneous boundary conditions and that $\nabla \cdot \boldsymbol{v} = 0$. Moreover, as it is often done in the background-flow method, we will choose $\boldsymbol{b}$ to satisfy the Euler equations, so that $\boldsymbol{b} \cdot \nabla \boldsymbol{b}$ is a gradient of some scalar. Consequently, $\langle \boldsymbol{v}, \boldsymbol{b} \cdot \nabla \boldsymbol{b}\rangle = 0$, which simplifies certain formulae. We will refer to $\boldsymbol{v}$ and $\boldsymbol{d}$ as perturbations, but it should be emphasised that they are perturbations from the background field $(\boldsymbol{b}, \boldsymbol{c}_b)$. Unlike in stability studies, $(\boldsymbol{b}, \boldsymbol{c}_b)$ is not required to be a solution of the governing equations.

The form of the auxiliary functional is motivated by the perturbation entropy functional introduced by Binns & Wynn (2024) for the global stability problem. In their setting, the reference state is the steady Couette solution, and the functional is used as a Lyapunov functional to prove decay towards that steady state. In the present work, we use the same structure, but replace the steady reference state by the general background pair $(\boldsymbol{b}, \boldsymbol{c}_b)$. Thus the functional below may be viewed as the background-flow analogue of the Binns & Wynn (2024) perturbation entropy: the background fields are not required to solve the governing equations, but are instead chosen to obtain the best possible dissipation bound.

Accordingly, we define the functional

$$V[\boldsymbol{u}, \boldsymbol{c}] = \frac{1}{2}\|\boldsymbol{v}\|^2 + \frac{1-\beta}{2\alpha Re\, Wi}\int_\Omega \operatorname{tr}(\boldsymbol{I} + \alpha \boldsymbol{d}) - 3 - \log\det(\boldsymbol{I} + \alpha \boldsymbol{d})\, \mathrm{d}V, \tag{4.2}$$

where $\boldsymbol{v} = \boldsymbol{u} - \boldsymbol{b}$, $\boldsymbol{d} = \boldsymbol{c} - \boldsymbol{c}_b$. The time-independent background fields $\boldsymbol{b}$, $\boldsymbol{c}_b$, together with the constant $\alpha > 0$, must all be specified to define V. The parameter α is used to ensure that $\boldsymbol{I} + \alpha \boldsymbol{d} \succ 0$, so that the logarithmic term is well defined. In the special case $\boldsymbol{c}_b = \boldsymbol{I}$ and $\alpha = 1$, the polymeric term in (4.2) coincides with the polymeric contribution to the total energy (2.10). For more general choices of $\boldsymbol{b}$ and $\boldsymbol{c}_b$, the functional (4.2) can

https://doi.org/10.1017/jfm.2026.11731 Published online by Cambridge University Press

be viewed as the sum of the kinetic energy of the velocity perturbation and a rescaled polymeric perturbation energy relative to the chosen background pair $(\boldsymbol{b}, \boldsymbol{c}_b)$.

To emphasise the 'energy like' properties of V, we now collect some of its important mathematical properties used in the subsequent analysis. First, the requirement that $\boldsymbol{I}+\alpha\boldsymbol{d}\succ 0$ ensures V is non-negative and $V[\boldsymbol{u}, \boldsymbol{c}]=0$ if and only if $(\boldsymbol{v}, \boldsymbol{d})=(\boldsymbol{0}, \boldsymbol{0})$ (Binns & Wynn 2024). Furthermore, V is bounded from above by dissipative terms in the perturbation variables via

$$0 \leq V[\boldsymbol{u}, \boldsymbol{c}] \leq C_p \frac{1}{2}\|\nabla \boldsymbol{v}\|^2 + \frac{1-\beta}{2\alpha Re\, Wi}\|\alpha \boldsymbol{d}\|^2_{\alpha \boldsymbol{d}} \qquad \forall\, (\boldsymbol{u}, \boldsymbol{c}) \in \mathcal{S}. \tag{4.3}$$

Here, C_p is a constant arising from the Poincaré inequality $\|\boldsymbol{v}\|^2 \leq C_p\|\nabla \boldsymbol{v}\|^2$, which holds since $\boldsymbol{v}$ has homogeneous boundary conditions. We have also introduced notation for the weighted inner product and norm

$$\langle \boldsymbol{A}, \boldsymbol{B}\rangle_{\boldsymbol{M}} := \int_\Omega \mathrm{tr}\left[\boldsymbol{A}^\top (\boldsymbol{I}+\boldsymbol{M})^{-1}\, \boldsymbol{B}\right] \mathrm{d}V, \qquad \|\boldsymbol{A}\|^2_{\boldsymbol{M}} = \langle \boldsymbol{A}, \boldsymbol{A}\rangle_{\boldsymbol{M}}, \tag{4.4}$$

defined for any vectors or matrices $\boldsymbol{A}$, $\boldsymbol{B}$ and any matrix satisfying $\boldsymbol{M}\succ -\boldsymbol{I}$, all of which may be spatially varying. With this notation, the standard L^2 norm defined in (2.11) can be written as $\|\cdot\|_{\boldsymbol{0}} = \|\cdot\|$, although we will continue to use the standard notation $\|\cdot\|$ throughout.

The system's total energy dissipation rate (2.14) can now be written as

$$\mathcal{E} = \frac{\beta}{Re}\|\nabla \boldsymbol{u}\|^2 + \frac{1-\beta}{2Re\, Wi^2}\|\boldsymbol{c}-\boldsymbol{I}\|^2_{\boldsymbol{c}-\boldsymbol{I}}, \tag{4.5}$$

highlighting the nature of $\boldsymbol{c}=\boldsymbol{I}$ as the un-deformed polymer states. An interesting feature of this polymeric term

$$\|\boldsymbol{c}-\boldsymbol{I}\|^2_{\boldsymbol{c}-\boldsymbol{I}} = \int_\Omega \mathrm{tr}\Big((\boldsymbol{c}-\boldsymbol{I})\boldsymbol{c}^{-1}(\boldsymbol{c}-\boldsymbol{I})\Big)\, \mathrm{d}V \tag{4.6}$$

is that close to the un-deformed configuration $\boldsymbol{c}\approx\boldsymbol{I}$ the norm behaves quadratically, yet for large deformations of the conformation tensor it scales linearly due to the presence of the inverse matrix in (4.6).

4.1. *Stability and dissipation of steady viscoelastic channel flow*

Before investigating the unsteady behaviour of the flow, we recall the known results on its stability. Binns & Wynn (2024) studied global stability of Oldroyd-B fluids using perturbation energies of the form (4.2) with

$$\boldsymbol{b} = \boldsymbol{b}_{steady} = y\boldsymbol{e}_x, \qquad \boldsymbol{c}_b = \boldsymbol{c}_{steady} = \begin{bmatrix} 1+2Wi^2 & Wi & 0 \\ Wi & 1 & 0 \\ 0 & 0 & 1 \end{bmatrix}, \tag{4.7}$$

taken as the laminar steady solution to the governing equations (2.5*a*–*c*). The key step in the analysis of Binns & Wynn (2024) is to show that if the non-dimensional parameters (β, Re, Wi) are sufficiently small, then α can be chosen in the definition of V (4.2) such that

$$\frac{\mathrm{d}V}{\mathrm{d}t} \leq -c\, V \tag{4.8}$$

holds along trajectories of (2.5*a*–*c*) for some constant $c>0$. Consequently, $V\to 0$ as $t\to\infty$ and one can conclude that the system is globally stable. That is, $(\boldsymbol{u}, \boldsymbol{c})\to(\boldsymbol{b}_{steady}, \boldsymbol{c}_{steady})$ as $t\to\infty$ from any arbitrary initial condition in $\mathcal{S}$.

https://doi.org/10.1017/jfm.2026.11731 Published online by Cambridge University Press

The specific parameter range in which this argument applies has the form

$$c_1\left(\frac{1-\beta}{1-Wi}\right)Wi + c_2 Re < \beta, \qquad 0 < Wi < 1, \tag{4.9}$$

where $c_1, c_2 > 0$ are positive constants. Within this parameter range the dissipation of the steady flow can be computed by substituting $\boldsymbol{b}_{steady}$ and $\boldsymbol{c}_{steady}$ into (2.14) to give $\overline{\mathcal{E}} = \mathcal{E}_{steady} = 1/Re$. This highlights an interesting feature of the Oldroyd-B model in the Couette geometry, in that the laminar viscoelastic dissipation rate is always equal to the corresponding Newtonian value.

4.2. *Perturbation energy and dissipation in unsteady viscoelastic channel flows*

Our aim now is to extend the parameter range (4.9) over which a quantifiable estimate on the size of $\overline{\mathcal{E}}$ can be proven. Since V is non-negative and vanishes only when $(\boldsymbol{v}, \boldsymbol{d}) = (\boldsymbol{0}, \boldsymbol{0})$, a Lyapunov decay estimate of the form (4.8) would imply $V(t) \to 0$ and hence convergence to the chosen reference state $(\boldsymbol{b}, \boldsymbol{c}_b)$; see for example Binns & Wynn (2024). Since we aim to make statements about the unsteady solutions of (2.5*a–c*), possibly far from the chosen background fields, we cannot in general expect such an estimate to hold. For the purpose of bounding time-averaged dissipation, it is sufficient instead to prove the weaker inequality

$$\frac{\mathrm{d}V}{\mathrm{d}t} \leq -c\,V + \gamma \tag{4.10}$$

for some constants $c, \gamma > 0$. This is important since it implies that V is bounded along trajectories of the system, meaning that condition (i) of Lemma 1 holds. Furthermore, the negative coefficient on the right-hand side of (4.10) gives some hope that the bounding condition (ii) of Lemma 1 can also hold.

To show how the inequality (4.10) may be proven, consider the following expression for $\mathrm{d}V/\mathrm{d}t$:

$$\begin{aligned}\frac{\mathrm{d}V}{\mathrm{d}t} = &\overbrace{-\frac{\beta}{2Re}\left(\|\nabla\boldsymbol{v}\|^2 + \|\nabla\boldsymbol{u}\|^2\right)}^{\text{fluid 'dissipation'}} \overbrace{-\frac{\alpha(1-\beta)}{2ReWi^2}\|\boldsymbol{d}\|^2_{\alpha\boldsymbol{d}}}^{\text{polymer 'dissipation'}} \overbrace{-\langle\boldsymbol{v}, \boldsymbol{v}\cdot\nabla\boldsymbol{b}\rangle + \frac{1-\beta}{ReWi}\langle\boldsymbol{v}, \nabla\cdot\boldsymbol{c}_b\rangle}^{\text{fluid/background coupling}} \\ &+ \overbrace{\frac{\alpha(1-\beta)}{ReWi}\langle\boldsymbol{d}(\boldsymbol{I}+\boldsymbol{d}), \nabla\boldsymbol{b}\rangle_{\alpha\boldsymbol{d}}}^{\text{polymer/background coupling}} \overbrace{-\frac{1-\beta}{ReWi}\left\langle\boldsymbol{d}, (\boldsymbol{I}-\alpha\boldsymbol{c}_b)\nabla\boldsymbol{v} + \frac{\alpha}{2}\boldsymbol{v}\cdot\nabla\boldsymbol{c}_b\right\rangle_{\alpha\boldsymbol{d}}}^{\text{polymer/fluid coupling}} \\ &+ \overbrace{\frac{\alpha(1-\beta)}{2ReWi}\left\langle\boldsymbol{d}, -\boldsymbol{b}\cdot\nabla\boldsymbol{c}_b + 2(\boldsymbol{c}_b-\boldsymbol{I})\nabla\boldsymbol{b} + \frac{1}{Wi}(\boldsymbol{I}-\boldsymbol{c}_b)\right\rangle_{\alpha\boldsymbol{d}} + \frac{\beta}{2Re}\|\nabla\boldsymbol{b}\|^2}^{\text{background 'constants'}}.\end{aligned} \tag{4.11}$$

For completeness, (4.11) is proven in Appendix A, but we refer the reader to Binns & Wynn (2024) for further details of the derivation.

The first two, dissipation-like, terms in (4.11) are negative. Whether (4.10) holds then depends on whether the other terms can be appropriately balanced by the 'dissipation' terms. We now discuss each of these terms, in order to give a high-level guide to the subsequent mathematical analysis in § 4.3.

https://doi.org/10.1017/jfm.2026.11731 Published online by Cambridge University Press

Fluid/background coupling:
The fluid/background coupling terms can be controlled from above by the 'perturbation dissipation' terms $\|\nabla \boldsymbol{v}\|^2$, provided that $\nabla \boldsymbol{b}$ and $\boldsymbol{c}_b$ are sufficiently small. For the first term, estimates of the form

$$\langle \boldsymbol{v}, \boldsymbol{v} \cdot \nabla \boldsymbol{b} \rangle \leq \frac{\text{const}}{Re} \|\nabla \boldsymbol{v}\|^2 \tag{4.12}$$

follow from the Poincaré inequality and are at the heart of the background-flow method for Newtonian fluids (see e.g. Doering & Constantin 1992). At low Reynolds numbers, the inequality can be satisfied for $\|\nabla b\| \approx \mathcal{O}(1)$, and it is important to note that $\|\nabla \boldsymbol{b}\| \geq 1$ must always hold, due to the assumption that $\boldsymbol{b}$ satisfies the Couette boundary conditions. However, at higher Reynolds numbers, the estimate (4.12) can only be enforced if $\nabla \boldsymbol{b}$ is concentrated in appropriately thin boundary layers, as indicated in figure 1. This exploits the homogeneous boundary conditions on $\boldsymbol{v}$ at the walls to control the left-hand side of (4.12). As will be detailed in § 4.3, this forces the choice

$$\|\nabla \boldsymbol{b}\| \geq \mathcal{O}(Re) \tag{4.13}$$

in the selection of the fluid-dependent part of the auxiliary functional V.

Polymer/background coupling:
Due to its dependence on $\boldsymbol{d}$, for (4.10) to hold this term must be controlled by the 'polymer dissipation'. This is possible if $\nabla \boldsymbol{b}$ is chosen to be small with respect to the magnitude of the polymer dissipation. However, given the constraint (4.13), this corresponds to requiring that the system parameters satisfy $ReWi \leq \mathcal{O}(1)$. This places a crucial restriction on our analysis: while arbitrarily large Reynolds numbers can be considered, rigorous bounds are only guaranteed for weakly elastic flows satisfying $Wi \lesssim Re^{-1}$. This restriction arises due to the assumption of only linear spring damping in the Oldroyd-B model, and is unlikely to be overcome without considering alternative constitutive models. Possible solutions to this barrier will be discussed later.

Polymer/fluid coupling:
This term is bilinear in $\boldsymbol{d}$ and $\nabla \boldsymbol{v}$ and can therefore be upper bounded by a combination of the fluid and polymeric 'dissipations' if $\boldsymbol{I} - \alpha \boldsymbol{c}_b$ and $\nabla \boldsymbol{c}_b$ are chosen to be sufficiently small. Again, there is no barrier to making such choices, other than modifying the value of the background constant terms, discussed above.

Background 'constants':
Although there is a dependence on the polymer perturbation $\boldsymbol{d}$, the first term in this expression has the form $\text{tr}(\boldsymbol{d}(\boldsymbol{I} + \alpha \boldsymbol{d})^{-1} f(\boldsymbol{b}, \boldsymbol{c}_b))$ and can therefore be upper bounded by a constant depending only on the background fields $\boldsymbol{b}$ and $\boldsymbol{c}_b$. Overall, the two terms considered here contribute only to the constant γ in (4.10).

Summary of the perturbation energy analysis:
Given the discussion of the non-dissipative terms in the perturbation energy equation (4.11), it is possible to prove that V is bounded along trajectories of the system, at least for viscoelastic flows with $ReWi \leq \mathcal{O}(1)$. Consequently, ΛV, and equivalently V, satisfies condition (i) of Lemma 1 and can therefore be used as a candidate for an auxiliary functional with which to satisfy the bounding condition (ii) of Lemma 1. To satisfy the

https://doi.org/10.1017/jfm.2026.11731 Published online by Cambridge University Press

bounding inequality, we will therefore search for constants Λ and κ such that

$$\mathcal{E} + \mathcal{L}_{\Lambda V} \leq \kappa \tag{4.14}$$

holds on all flow/polymer fields in $\mathcal{S}$.

4.3. *An analytical bound on dissipation*

The perturbation energy equation (4.11) can be significantly simplified by making the choices $\alpha = 1$, $\boldsymbol{c}_b = \boldsymbol{I}$, which eliminate all $\boldsymbol{c}_b$-dependent contributions to the terms on the right-hand side of (4.11). We also choose $\boldsymbol{b} = b(y)\,\boldsymbol{e}_x$ with

$$b(y) = \begin{cases} \dfrac{1}{2\delta}y, & 0 \leq y < \delta, \\ \dfrac{1}{2}, & \delta \leq y \leq 1-\delta, \\ \dfrac{1}{2} + \dfrac{1}{2\delta}(y-(1-\delta)), & 1-\delta < y \leq 1. \end{cases} \tag{4.15}$$

This corresponds to the 'background profile' used in the classical analysis of dissipation bounds for Newtonian Couette flow, indicated in figure 1. While there may be potential for optimisation, such choices will allow us to present the main result more clearly. In particular, (4.11) reduces to

$$\begin{aligned} \frac{\mathrm{d}V}{\mathrm{d}t} = &-\frac{\beta}{2Re}\left(\|\nabla \boldsymbol{v}\|^2 + \|\nabla \boldsymbol{u}\|^2\right) - \frac{1-\beta}{2ReWi^2}\,\|\boldsymbol{d}\|^2_{\boldsymbol{d}} \\ &+ \int_\Omega b' v_x v_y \,\mathrm{d}V + \frac{1-\beta}{ReWi}\,\langle \boldsymbol{d}(\boldsymbol{I}+\boldsymbol{d}), \nabla \boldsymbol{b}\rangle_{\boldsymbol{d}} + \frac{\beta}{2Re}\,\|\nabla \boldsymbol{b}\|_2^2\,, \end{aligned} \tag{4.16}$$

where $b' = \mathrm{d}b(y)/\mathrm{d}y$ denotes the derivative of the scalar background profile $b(y)$ in $\boldsymbol{b} = b(y)\,\boldsymbol{e}_x$ with respect to the wall-normal coordinate y. Now recall from (4.5) that the expression for dissipation can be written as

$$\mathcal{E} = \frac{\beta}{Re}\|\nabla \boldsymbol{u}\|^2 + \frac{1-\beta}{2ReWi^2}\|\boldsymbol{c}-\boldsymbol{I}\|^2_{\boldsymbol{c}-\boldsymbol{I}}. \tag{4.17}$$

This can be compared with the dissipative terms in $\mathrm{d}V/\mathrm{d}t$ by noticing that, with the choice $\boldsymbol{c} = \boldsymbol{I} + \boldsymbol{d}$, we have that

$$\|\boldsymbol{d}\|^2_{\boldsymbol{d}} = \|\boldsymbol{c}-\boldsymbol{I}\|^2_{\boldsymbol{c}-\boldsymbol{I}}. \tag{4.18}$$

We now seek to show that (4.14) holds for some constants Λ, κ. Using (4.16)

$$\begin{aligned} \mathcal{E} + \mathcal{L}_{\Lambda V} &= \mathcal{E} + \Lambda\frac{\mathrm{d}V}{\mathrm{d}t} \\ &= \Lambda\left(-\frac{\beta}{2Re}\|\nabla \boldsymbol{v}\|^2 - \int_\Omega b' v_x v_y \,\mathrm{d}V + \frac{\beta}{2Re}\|\nabla \boldsymbol{b}\|^2\right) \\ &\quad + \frac{(2-\Lambda)\beta}{2Re}\|\nabla \boldsymbol{u}\|^2 \\ &\quad + \Lambda\frac{1-\beta}{ReWi}\int_\Omega b' c_{xy}\,\mathrm{d}V - \frac{(\Lambda-1)(1-\beta)}{2ReWi^2}\|\boldsymbol{c}-\boldsymbol{I}\|^2_{\boldsymbol{c}-\boldsymbol{I}}. \end{aligned} \tag{4.19}$$

To begin, we upper bound the first bracketed term in (4.19). Since b' is supported only in boundary layers of width δ, no-slip boundary conditions, Young's inequality and

https://doi.org/10.1017/jfm.2026.11731 Published online by Cambridge University Press

incompressibility imply that (Doering & Constantin 1992)

$$\begin{aligned}\left|\int_\Omega b' v_x v_y \,\mathrm{d}V\right| &\leq \frac{1}{2\delta}\left(\left|\int_0^{\Gamma_z}\int_0^{\delta}\int_0^{\Gamma_x} v_x v_y \,\mathrm{d}x\,\mathrm{d}y\,\mathrm{d}z\right| + \left|\int_0^{\Gamma_z}\int_{1-\delta}^{1}\int_0^{\Gamma_x} v_x v_y \,\mathrm{d}x\,\mathrm{d}y\,\mathrm{d}z\right|\right)\\ &\leq \frac{\delta}{4}\left\|\frac{\partial v_x}{\partial y}\right\|\left\|\frac{\partial v_y}{\partial y}\right\|\\ &\leq \frac{\delta}{4}\left(\frac{1}{2\sqrt{2}}\left\|\frac{\partial v_x}{\partial y}\right\|^2 + \frac{\sqrt{2}}{2}\left\|\frac{\partial v_y}{\partial y}\right\|^2\right) \leq \frac{\delta}{8\sqrt{2}}\left\|\boldsymbol{\nabla v}\right\|^2. \end{aligned} \tag{4.20}$$

Consequently, $\int_\Omega b' v_x v_y \,\mathrm{d}V$ can be upper bounded by the 'perturbation dissipation' if δ is chosen to be sufficiently small. Namely, if

$$0 < \delta \leq \min\left\{\frac{1}{2}, \frac{4\sqrt{2}\beta}{Re}\right\}, \tag{4.21}$$

then

$$-\frac{\beta}{2Re}\left\|\boldsymbol{\nabla v}\right\|^2 - \int_\Omega b' v_x v_y \,\mathrm{d}V \leq 0. \tag{4.22}$$

If we make the additional assumption that

$$\Lambda \geq 2, \tag{4.23}$$

so that the term involving $\|\boldsymbol{\nabla u}\|^2$ in (4.19) can be upper bounded by zero, and use that $\|\boldsymbol{\nabla b}\|^2 = 1/(2\delta)$, it follows from (4.19) and (4.22) that

$$\mathcal{E} + \mathcal{L}_{\Lambda V} \leq \frac{\Lambda\beta}{4\delta Re} + \Lambda\frac{1-\beta}{Re\,Wi}\int_\Omega b' c_{xy}\,\mathrm{d}V - \frac{(\Lambda-1)(1-\beta)}{2Re\,Wi^2}\left\|\boldsymbol{c}-\boldsymbol{I}\right\|^2_{\boldsymbol{c}-\boldsymbol{I}}. \tag{4.24}$$

To complete the proof of the bound, i.e. to upper bound (4.24) by a constant κ, it is necessary to estimate the sign-indefinite term $\int_\Omega b' c_{xy}\,\mathrm{d}V$. This corresponds to the production of energy via polymer stretching induced by the 'background' shear, which must be appropriately controlled by the polymeric energy dissipation arising from the spring damping in the Oldroyd-B model. To see why this is possible, the following fact, which acts similarly to a Young-type inequality for off-diagonal elements of positive-definite matrices, is required.

LEMMA 2. *Let $\boldsymbol{c}$ be a 3×3 symmetric positive-definite matrix. Then*

$$\left|c_{xy}\right| \leq \frac{a}{2}\left\|\boldsymbol{c}-\boldsymbol{I}\right\|^2_{\boldsymbol{c}-\boldsymbol{I}} + \frac{2-\sqrt{2}}{a}, \tag{4.25}$$

holds for any $a \geq 1$.

The proof of this lemma is given in Appendix B.

In terms of the physical interpretation of the conformation tensor, this lemma implies that the cross-correlation of polymer stretching in the $\boldsymbol{e}_x$ and $\boldsymbol{e}_y$ directions cannot exceed the sum of the variances of the polymer deformations in each direction.

https://doi.org/10.1017/jfm.2026.11731 Published online by Cambridge University Press

To make use of Lemma 2, we let $\Omega_\delta := \{\Omega : y \in [0, \delta] \cup [1-\delta, 1]\}$ and again use that b' is supported in boundary layers of width δ to show that

$$\begin{aligned}\Lambda\frac{1-\beta}{Re\,Wi}\int_\Omega b'c_{xy}\,\mathrm{d}V &\le \frac{\Lambda(1-\beta)}{2\delta Re\,Wi}\int_{\Omega_\delta}\left|c_{xy}\right|\,\mathrm{d}V \\ &\le \frac{\Lambda(1-\beta)}{2\delta Re\,Wi}\left[\frac{a}{2}\|\boldsymbol{c}-\boldsymbol{I}\|^2_{\boldsymbol{c}-\boldsymbol{I}}+\frac{2\delta\left(2-\sqrt{2}\right)}{a}\right],\end{aligned} \tag{4.26}$$

which holds for any $a \ge 1$. This freedom is useful, since if a is chosen to satisfy

$$1 \le a \le \frac{2\delta(1-\Lambda^{-1})}{Wi} \tag{4.27}$$

then the first term on the right-hand side of (4.26) can be upper bounded by the final negative term in (4.24). In summary, we have proven that if the three constraints (4.21), (4.23) and (4.27) hold on the parameters δ, Λ and a then we have the upper bound

$$\mathcal{E}+\mathcal{L}_{\Lambda V} \le \frac{\Lambda\beta}{4\delta Re}+\left(2-\sqrt{2}\right)\frac{\Lambda(1-\beta)}{a\,Re\,Wi}. \tag{4.28}$$

This shows that condition (ii) of Lemma 1 holds for the auxiliary functional ΛV.

One possible choice for the parameters is given by

$$\delta=\min\left\{\frac{1}{2},\frac{4\sqrt{2}\beta}{Re}\right\},\qquad \Lambda=\frac{2}{1-Wi},\qquad a=\frac{2\delta}{Wi}\left(1-\frac{1}{\Lambda}\right). \tag{4.29}$$

The choice of Λ is made so that the polymer-production term $b'c_{xy}$ can be controlled by the dissipation in (4.24), and already requires $0 < Wi < 1$. These parameters satisfy the required constraints (4.21), (4.23) and (4.27) provided $a \ge 1$. This final condition is equivalent to

$$a=\delta\left(1+Wi^{-1}\right)\ge 1 \tag{4.30}$$

which places an inherent restriction on the range of system parameters (Re, Wi, β) to which the result can apply. Since $\delta \le 1/2$, the condition $a \ge 1$ can only hold if $Wi < 1$. At larger Reynolds numbers when δ is small, we have the extra restriction $Re < 4\sqrt{2}\beta(1+Wi^{-1})$. We collect these observations in the main analytical result of the paper.

THEOREM 1. *Let* $0 < Wi < 1$ *and* $0 < \beta < 1$. *If*

$$0 < Re < 4\sqrt{2}\beta\left(1+Wi^{-1}\right), \tag{4.31}$$

then the upper bound on the infinite-time-averaged energy dissipation rate

$$\overline{\mathcal{E}} \le \left(\frac{1}{1-Wi}\right)\left(\frac{1}{8\sqrt{2}}+\frac{(\sqrt{2}-1)(1-\beta)}{2\beta(1+Wi)}\right)\max\left\{1,\frac{8\sqrt{2}\beta}{Re}\right\} \tag{4.32}$$

must hold for any solution to the Oldroyd-B equations (2.5) whose initial condition belongs to the admissible set $\mathcal{S}$ *given by (2.9).*

Proof. This requires checking the technical conditions of Lemma 1, as detailed in Appendix C. □

https://doi.org/10.1017/jfm.2026.11731 Published online by Cambridge University Press

5. Discussion

Theorem 1 gives conditions under which quantitative upper bounds on the time-averaged energy dissipation rate $\overline{\mathcal{E}}$ can be proven for solutions to the Oldroyd-B equations (2.5*a*–*c*). Given (4.31), the bound holds at arbitrarily high Reynolds numbers if Wi is sufficiently small and β is bounded away from zero. We first discuss the relation of these bounds to those available in the Newtonian setting.

When $Wi \approx 0$, $\beta \approx 1$, at leading order the bound (4.32) becomes

$$\overline{\mathcal{E}} \leq \underbrace{\frac{1}{8\sqrt{2}}}_{\text{'Newtonian'}} + \frac{Wi}{8\sqrt{2}} + \frac{\sqrt{2}-1}{2}(1-\beta), \qquad \text{for} \quad 8\sqrt{2}\beta \leq Re \lesssim \frac{1}{Wi}, \tag{5.1}$$

which naturally extends the classical upper bound $\overline{\mathcal{E}} \leq (8\sqrt{2})^{-1}$ proven by Doering & Constantin (1992) for Newtonian Couette flow for $Re \gg 1$. In the viscoelastic setting, (5.1) suggests that weakly elastic polymeric perturbations to the Newtonian base case are subtly destabilising, in the sense that the provable bounds on dissipation are larger than those available for the corresponding Newtonian flow. Despite this, the conditions under which Theorem 1 holds, as proven in Appendix C, explicitly rule out the possibility of a blow-up of the Oldroyd-B fluid flow for cases $Re \sim Wi^{-1} \gg 1$ in which one would expect weakly elastic turbulence. This may be of interest, given the well-known challenges involved with numerically simulating viscoelastic fluid flows. If one observes a blow-up at these parameter values, then it is numerical, not physical.

At low Reynolds numbers, the bound (4.32) approaches $\overline{\mathcal{E}} \leq 1/Re$ when $Wi \approx 0$, $\beta \approx 1$. As noted previously, this corresponds to the dissipation rate of the steady solution to the governing equations. While natural, this highlights an interesting deficiency of the main result: the proven bound does not precisely agree with the 'correct' dissipation rate of the steady solution unless we are in the limiting Newtonian case $Wi = 0$, $\beta = 1$.

This sub-optimality arises for a simple reason. In the proof of Theorem 1, we analyse the 'energy' of perturbations from the background fields $\boldsymbol{b} = b(y)\boldsymbol{e}_x$ and $\boldsymbol{c}_b = \boldsymbol{I}$. For the chosen construction of b, at low Reynolds numbers $b(y) \equiv y$, which agrees with the steady solution for the fluid solvent. However, the fixed choice $\boldsymbol{c}_b = \boldsymbol{I}$ does not correspond to the steady polymeric field other than in the limiting case $Wi = 0$ (see (4.7)). While convenient for the presentation of the analysis, this choice is not optimal for 'small' parameter values, and in particular those satisfying the conditions (4.9) in which the flow is known to be globally stable.

A natural way to remove this suboptimal behaviour is to follow the approach of global stability analysis of Binns & Wynn (2024) and make the choices $\boldsymbol{b} = \boldsymbol{b}_{steady}$ and $\boldsymbol{c}_b = \boldsymbol{c}_{steady}$ in our bounding analysis. The following result, whose proof is given in Appendix D, shows that this gives the desired improvement.

THEOREM 2. *Suppose that V is given by (4.2) with $\boldsymbol{b} = \boldsymbol{b}_{steady}$ and $\boldsymbol{c}_b = \boldsymbol{c}_{steady}$. Then there exists a constant $c > 0$, independent of Λ, such that*

$$\overline{\mathcal{E} + \Lambda \frac{\mathrm{d}V}{\mathrm{d}t}} \leq \frac{1}{Re} + \frac{c}{\Lambda}, \qquad \Lambda \gg 1, \tag{5.2}$$

whenever the system parameters satisfy (4.9).

An immediate corollary of Theorem 2 is that – since Λ can be chosen to be arbitrarily large – the steady dissipation rate $\overline{\mathcal{E}} \leq 1/Re$ is provable with the auxiliary-functional method. Thus we have a unified approach to proving bounds for both stable and unstable

https://doi.org/10.1017/jfm.2026.11731 Published online by Cambridge University Press

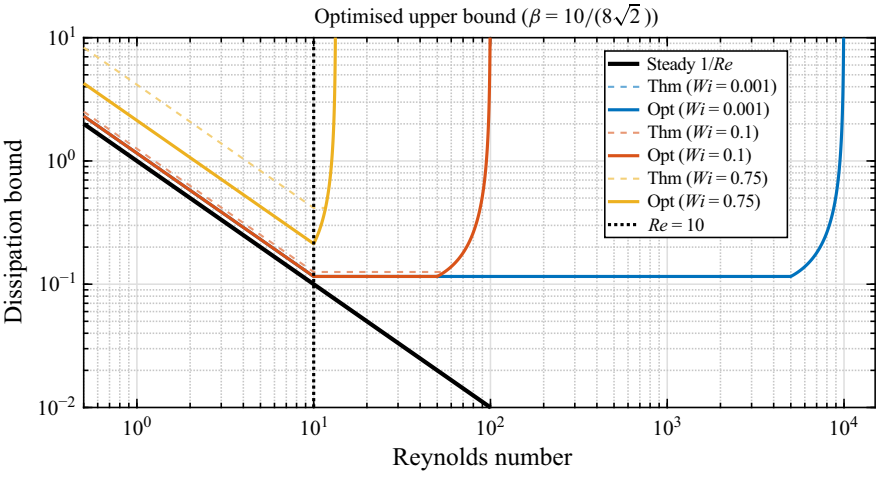


Figure 2. The scaling with Re of the upper bounds on dissipation $\overline{\mathcal{E}}$ obtained from Theorem 1 (dashed lines) and the 'optimal' bounds found by solving (5.3) (solid lines) at selected Weissenberg numbers, for $\beta = 10/(8\sqrt{2})$. The dissipation rate $1/Re$ of the steady solution is shown with a solid black line. The critical Reynolds number $Re = 8\sqrt{2}\beta = 10$ separating the two cases of Theorem 1 is indicated with a vertical dotted line.

flow conditions. Given this observation, it is interesting to note that the choices of polymeric 'background' field in Theorems 1 and 2 represent natural, yet extreme, ends of the possible choices for $\boldsymbol{c}_b$. In the low Reynolds and Weissenberg number regimes addressed by Theorem 2, the steady solution $\boldsymbol{c}_b = \boldsymbol{c}_{steady}$ is the natural choice. In contrast, the bound (4.32), which is applicable at high Reynolds numbers, is obtained using $\boldsymbol{c}_b = \boldsymbol{I}$. This corresponds to the expected orientation of polymers in the bulk of a 'well-mixed' turbulent flow. One could reasonably expect to obtain improved bounds at intermediate parameter values by choosing $\boldsymbol{c}_b$ as an appropriate interpolation between $\boldsymbol{I}$ and $\boldsymbol{c}_{steady}$. However, implementing this idea is technically challenging due to the large parameter space (e.g. the choice of α, a, $\boldsymbol{b}$, $\boldsymbol{c}_b$ and Λ) and the 'asymptotic' behaviour of the balancing parameter Λ observed in Theorem 2.

We reserve a full numerical investigation of this question for future work. Here, we present only a numerically optimal implementation of the proof of Theorem 1, indicating the best bounds available by choosing: $\boldsymbol{c}_b = \boldsymbol{I}$, $\boldsymbol{b} = b(y)\,\boldsymbol{e}_x$ with b given by (4.15), and optimising over the parameters a, δ, Λ. For each choice of (Re, Wi, β) this corresponds to solving the constrained optimisation problem

$$\begin{aligned} \min_{a,\delta,\Lambda} \quad & \frac{\Lambda\beta}{4\delta Re} + \left(2-\sqrt{2}\right)\frac{\Lambda(1-\beta)}{a\,Re\,Wi} \\ \text{subject to} \quad & 0 < \delta \le \frac{1}{2}, \quad a \ge 1, \quad \Lambda \ge 2, \\ & \delta \le \frac{4\sqrt{2}\beta}{Re}, \quad a \le \frac{2\delta}{Wi}\left(1-\Lambda^{-1}\right). \end{aligned} \tag{5.3}$$

Figure 2 compares the analytical bound derived in Theorem 1 (dashed lines) with the tighter bounds (solid lines) obtained by solving (5.3). The improvement given by (5.3) is greater at higher Weissenberg numbers (e.g. $Wi = 0.75$), largely due to the conservative choice $\Lambda = 2/(1 - Wi)$ taken in the proof of Theorem 1: the bound scales linearly with Λ and the optimal choice for $\Lambda \gg 1$ is approximately half this value. Figure 2 also shows that

https://doi.org/10.1017/jfm.2026.11731 Published online by Cambridge University Press

for $Re \leq 10$ there is always a finite gap between the steady dissipation rate $1/Re$ and the best bound obtained by solving (5.3). This clearly demonstrates the previous observation that the choice $\boldsymbol{c}_b = \boldsymbol{I}$ is not optimal for some parameter values: for any $0 < \beta < 1$, $Wi < 1$ there exists sufficiently small Reynolds number such that the system parameters satisfy (4.9) and so, by Theorem 2, the bound $1/Re$ is provable with $\boldsymbol{c}_b = \boldsymbol{c}_{steady}$.

The discussion so far indicates that our results on boundedness and stability of the Oldroyd-B model in Couette flow appear natural in the context of extending what is known in the Newtonian case to weakly elastic regimes. A key limitation, however, is the restriction to small Weissenberg numbers satisfying $0 < Wi < 1$, which arises from the restrictions $a \geq 1$, $\delta \leq 1/2$. While extending the rigorous bound presented here to regimes ($Wi > 1$) in which polymer-induced drag reduction is known to occur remains a significant open challenge, our analysis nonetheless offers insights into physical reasons for this restriction, and possible ways to overcome it. The limited parameter range over which Theorem 1 is admissible occurs due to 'worst-case' polymer configurations that maximise the 'production' term $\int_\Omega b' c_{xy}\, \mathrm{d}V$ relative to the 'dissipative' effect of the linear spring damping in the Oldroyd-B model, i.e. those which saturate the key estimate of c_{xy} in Lemma 2.

One may therefore ask in what manner this estimate is conservative, either for Oldroyd-B or for other constitutive models. An interesting observation is that, under mild assumptions explained in Appendix E, the behaviour of the conformation tensor at the wall satisfies a much stronger upper estimate than that given by Lemma 2, namely,

$$\overline{c_{xy}^2\big|_{wall}} \leq \frac{1}{2}\overline{\mathrm{tr}\left((\boldsymbol{c}-\boldsymbol{I})\boldsymbol{c}^{-1}(\boldsymbol{c}-\boldsymbol{I})\right)\big|_{wall}}. \tag{5.4}$$

The fact that c_{xy}^2 is upper bounded here, as opposed to $|c_{xy}|$ in Lemma 2, gives more control over the polymer terms than is provable in our current analysis, albeit only at the wall. This extra control is potentially significant, since if it were the case that (5.4) held in a boundary layer of width $\delta = 4\sqrt{2}\beta/Re$, then an upper bound on dissipation $\overline{\mathcal{E}} \leq 1/(8\sqrt{2}\beta)$ would hold for any Re, $Wi > 0$ (this can be proven by adapting Theorem 1 with the choices $\Lambda = 2$, $\delta = 4\sqrt{2}\beta/Re$). In this hypothetical scenario, the behaviour of the Oldroyd-B model would have, provably, a comparable upper bound on dissipation to what can be shown in the Newtonian case.

The physical reason for (5.4) is that the presence of the walls impedes polymer stretching in the wall-normal direction so that, after an initial transient, $c_{yy}\big|_{wall} = 1$. This restriction implies that, at the wall, the conformation tensor responds as if it is in a steady shear flow driven by the mean wall shear stress of the solvent. Since c_{yy} is fixed and $\det \boldsymbol{c} > 0$, it then follows that the square of the shear component c_{xy}^2 is upper bounded by the polymeric potential energy (note, for example, that the steady solution $\boldsymbol{c}_{steady}$ from (4.7) satisfies the inequality (5.4)). From the argument in the previous paragraph, if even a bound of the form $c_{yy} \leq 1 + \rho$ was available in a boundary layer near the wall, then one could prove energy boundedness and dissipation bounds for the Oldroyd-B model at arbitrary Weissenberg numbers.

It appears to be an open question as to whether such a bound on c_{yy} holds for solutions to the Oldroyd-B model in the Couette geometry. For arbitrary flows, the answer is false since extensional flows on unbounded domains can cause arbitrarily large polymer deformations. For channel flows, while the presence of the walls necessarily prevents such pathological behaviour, it is unclear how to formally use this observation to make physically meaningful predictions. An alternative approach is to apply the present auxiliary-functional framework to other upper-convected Maxwell-type models.

https://doi.org/10.1017/jfm.2026.11731 Published online by Cambridge University Press

The construction is not tied to the particular Oldroyd-B free energy in (2.10), but rather to the existence of an energy balance of the form (2.13) with a non-negative polymer dissipation. For a different constitutive model, one would replace the Oldroyd-B polymeric entropy term in V by the corresponding free energy for that model, while retaining the same background-flow approach: decompose the conformation tensor relative to a chosen background state, and control the resulting polymer-production terms using the model's polymer dissipation. This includes, for example, finitely extensible models such as FENE-P and finitely extensible nonlinear elastic-Chilcott–Rallison, and nonlinearly damped models such as the Giesekus and Phan–Thien–Tanner models. In these models, finite extensibility or nonlinear damping provides additional control over large polymer deformations, and therefore alters the production–dissipation balance responsible for the restriction in Theorem 1.

Finally, from a purely methodological perspective, this paper demonstrates that the background-flow method can be rigorously extended to systems where the energy is not quadratic. In Newtonian applications, the background-flow method can be interpreted neatly in the language of auxiliary functionals: one searches for a functional V obtained by adding a linear perturbation to the quadratic energy, and satisfying the condition of Lemma 1. In the non-Newtonian setting, the non-quadratic nature of energy means that such a neat characterisation no longer holds. This observation is at the heart of the methodological challenges, discussed above, of picking an appropriate background polymer field. We note that, while some attempt has been made to introduce a quadratic form of polymer energy (Balci *et al.* 2011), this approach renders the right-hand side of the constitutive equation non-polynomial, and it is unclear if this simplifies the analysis. The present work establishes one such non-polynomial auxiliary-functional construction for Oldroyd-B fluids, and its extension to a broader class of upper-convected Maxwell-type models will be investigated in future work.

6. Conclusion

In this paper, using a non-polynomial auxiliary functional, we prove the first mathematically rigorous upper bound on the infinite-time-averaged energy dissipation rate in plane Couette flow of Oldroyd-B fluids. The bound is valid for arbitrarily large Reynolds numbers given a sufficiently small Weissenberg number. The bound holds within a certain region in the parameter space, and depends explicitly on the system parameters. In the Newtonian limit, the bound coincides with the classical Newtonian result. For flow parameters for which the flow can be proven steady, we obtain a tighter bound by picking a different auxiliary functional.

We also provide the first known proof that the total energy of the fluid is uniformly bounded in time, if bounded initially, for a region of flow parameters wider than the region within which the flow has been proven globally stable. Because the proof is mathematically rigorous, this result can help in separating potentially genuine flow behaviour from high-Weissenberg-number-problem-type numerical artefacts and singularities.

One central contribution is the demonstration of how the background-flow method can be extended to cases where energy is no longer quadratic, or even polynomial. To our knowledge, this is the first use of a non-quadratic auxiliary functional in obtaining rigorous bounds for Navier–Stokes-related problems. The method used provides a basis for bounding non-polynomial observables in dynamical systems, particularly when a non-polynomial Lyapunov functional is already known.

These outputs – extending the background-flow method to cases when energy is not polynomial, the first application of non-polynomial auxiliary functionals in fluid

https://doi.org/10.1017/jfm.2026.11731 Published online by Cambridge University Press

mechanics, the rigorous upper bound on the energy dissipation rate and the proof of the boundedness of energy in Oldroyd-B shear flow in a certain parameter range – are the main contributions of this work.

Declaration of interests. The authors report no conflict of interest.

Appendix A. An identity for $\mathrm{d}V/\mathrm{d}t$

Consider the auxiliary functional

$$V = \frac{1}{2}\|\boldsymbol{v}\|^2 + \frac{1-\beta}{2\alpha Re\, Wi}\int_\Omega \mathrm{tr}(\boldsymbol{I}+\alpha\boldsymbol{d}) - 3 - \log\det(\boldsymbol{I}+\alpha\boldsymbol{d})\,\mathrm{d}V. \tag{A1}$$

To differentiate the polymeric component of V, we use the Jacobi formula $(\partial/\partial t)\log\det(\boldsymbol{A}) = \mathrm{tr}(\boldsymbol{A}^{-1}(\partial\boldsymbol{A}/\partial t))$ and the identity $\boldsymbol{I} - (\boldsymbol{I}+\alpha\boldsymbol{d})^{-1} = (\boldsymbol{I}+\alpha\boldsymbol{d})^{-1}\alpha\boldsymbol{d}$ to obtain

$$\frac{\mathrm{d}V}{\mathrm{d}t} = \left\langle \boldsymbol{v}, \frac{\partial\boldsymbol{v}}{\partial t}\right\rangle + \frac{1-\beta}{2Re\, Wi}\left\langle \alpha\boldsymbol{d}, \frac{\partial\boldsymbol{d}}{\partial t}\right\rangle_{\alpha\boldsymbol{d}} \tag{A2}$$

along trajectories of the system (2.5*a*–*c*).

Considering the fluid part of (A2) first, we use (2.5*a*) and follow the standard approach of integrating by parts, using incompressibility and the homogeneous/periodic boundary conditions on $\boldsymbol{v}$, to obtain

$$\left\langle \boldsymbol{v}, \frac{\partial\boldsymbol{v}}{\partial t}\right\rangle = -\frac{\beta}{Re}\|\nabla\boldsymbol{v}\|^2 - \langle \boldsymbol{v}, \boldsymbol{v}\cdot\nabla\boldsymbol{b}\rangle - \frac{1-\beta}{Re\, Wi}\langle \boldsymbol{d}, \nabla\boldsymbol{v}\rangle + \frac{\beta}{Re}\left\langle \boldsymbol{v}, \nabla^2\boldsymbol{b}\right\rangle + \frac{1-\beta}{Re\, Wi}\langle \boldsymbol{v}, \nabla\cdot\boldsymbol{c}_b\rangle. \tag{A3}$$

To evaluate the polymeric contribution to $\mathrm{d}V/\mathrm{d}t$, we first use (2.5*c*) to get

$$\left\langle \boldsymbol{d}, \frac{\partial\boldsymbol{d}}{\partial t}\right\rangle_{\alpha\boldsymbol{d}} = \left\langle \boldsymbol{d}, -(\boldsymbol{u}\cdot\nabla\boldsymbol{c}) + s(\boldsymbol{c}, \nabla\boldsymbol{u}) + \frac{1}{Wi}(\boldsymbol{I}-\boldsymbol{c})\right\rangle_{\alpha\boldsymbol{d}}, \tag{A4}$$

where $s(\boldsymbol{a}, \boldsymbol{b}) := \boldsymbol{a}\cdot\boldsymbol{b} + \boldsymbol{b}^\top\cdot\boldsymbol{a}^\top$. Since $\boldsymbol{u}$ is incompressible, it follows that $\langle \boldsymbol{d}, (\boldsymbol{u}\cdot\nabla)\boldsymbol{d}\rangle_{\alpha\boldsymbol{d}} = 0$. Using this and substituting $\boldsymbol{c} = \boldsymbol{c}_b + \boldsymbol{d}$, $\boldsymbol{u} = \boldsymbol{b} + \boldsymbol{v}$ into the above equation gives

$$\begin{aligned}\left\langle \boldsymbol{d}, \frac{\partial\boldsymbol{d}}{\partial t}\right\rangle_{\alpha\boldsymbol{d}} = &-\langle \boldsymbol{d}, (\boldsymbol{v}\cdot\nabla)\boldsymbol{c}_b\rangle_{\alpha\boldsymbol{d}} + \left\langle \boldsymbol{d}, -(\boldsymbol{b}\cdot\nabla)\boldsymbol{c}_b + s(\boldsymbol{c}_b, \nabla\boldsymbol{b}) + \frac{1}{Wi}(\boldsymbol{I}-\boldsymbol{c}_b)\right\rangle_{\alpha\boldsymbol{d}} \\ &+ \langle \boldsymbol{d}, s(\boldsymbol{d}, \nabla\boldsymbol{v}) + s(\boldsymbol{c}_b, \nabla\boldsymbol{v}) + s(\boldsymbol{d}, \nabla\boldsymbol{b})\rangle_{\alpha\boldsymbol{d}} - \frac{1}{Wi}\|\boldsymbol{d}\|^2_{\alpha\boldsymbol{d}}.\end{aligned} \tag{A5}$$

The term $\langle \boldsymbol{d}, s(\boldsymbol{d}, \nabla\boldsymbol{v})\rangle_{\alpha\boldsymbol{d}}$ is problematic when attempting to upper bound $\mathrm{d}V/\mathrm{d}t$, due to the fact that it is 'quadratic' in the perturbation variables, as opposed to the linear spring damping available in the Oldroyd-B model. However, this term can be simplified when combined with the $\langle \boldsymbol{d}, \nabla\boldsymbol{v}\rangle$ term from (A3) in the following way:

$$-\langle \boldsymbol{d}, \nabla\boldsymbol{v}\rangle + \frac{\alpha}{2}\langle \boldsymbol{d}, s(\boldsymbol{d}, \nabla\boldsymbol{v})\rangle_{\alpha\boldsymbol{d}} = -\langle (\boldsymbol{I}+\alpha\boldsymbol{d})\boldsymbol{d}, \nabla\boldsymbol{v}\rangle_{\alpha\boldsymbol{d}} + \left\langle \alpha\boldsymbol{d}^2, \nabla\boldsymbol{v}\right\rangle_{\alpha\boldsymbol{d}} = -\langle \boldsymbol{d}, \nabla\boldsymbol{v}\rangle_{\alpha\boldsymbol{d}}. \tag{A6}$$

https://doi.org/10.1017/jfm.2026.11731 Published online by Cambridge University Press

Substituting (A3) and (A5) into (A2) and using the identity (A6) then gives

$$\begin{aligned}\frac{\mathrm{d}V}{\mathrm{d}t}=&-\frac{\beta}{Re}\,\|\nabla \boldsymbol{v}\|^2-\frac{\alpha(1-\beta)}{2ReWi^2}\|\boldsymbol{d}\|^2_{\alpha\boldsymbol{d}}-\langle \boldsymbol{v},\,\boldsymbol{v}\cdot\nabla\boldsymbol{b}\rangle+\frac{\beta}{Re}\left\langle \boldsymbol{v},\,\nabla^2\boldsymbol{b}\right\rangle+\frac{1-\beta}{ReWi}\,\langle \boldsymbol{v},\,\nabla\cdot\boldsymbol{c}_b\rangle\,,\\&+\frac{\alpha(1-\beta)}{ReWi}\left\langle \boldsymbol{d}^2,\,\nabla\boldsymbol{b}\right\rangle_{\alpha\boldsymbol{d}}-\frac{1-\beta}{ReWi}\left\langle \boldsymbol{d},\,(\boldsymbol{I}-\alpha\boldsymbol{c}_b)\nabla\boldsymbol{v}+\frac{\alpha}{2}(\boldsymbol{v}\cdot\nabla)\boldsymbol{c}_b\right\rangle_{\alpha\boldsymbol{d}}\\&+\frac{\alpha(1-\beta)}{2ReWi}\left\langle \boldsymbol{d},\,-(\boldsymbol{b}\cdot\nabla)\boldsymbol{c}_b+s(\boldsymbol{c}_b,\,\nabla\boldsymbol{b})+\frac{1}{Wi}(\boldsymbol{I}-\boldsymbol{c}_b)\right\rangle_{\alpha\boldsymbol{d}}.\end{aligned}\tag{A7}$$

Since $\boldsymbol{v}$ satisfies homogeneous/periodic boundary conditions

$$\|\nabla\boldsymbol{u}\|^2=\|\nabla\boldsymbol{v}\|^2+2\,\langle\nabla\boldsymbol{b},\,\nabla\boldsymbol{v}\rangle+\|\nabla\boldsymbol{b}\|^2=\|\nabla\boldsymbol{v}\|^2-2\left\langle \boldsymbol{v},\,\nabla^2\boldsymbol{b}\right\rangle+\|\nabla\boldsymbol{b}\|^2\,.\tag{A8}$$

Using the above identity we can split $\|\nabla\boldsymbol{v}\|^2$ into two parts and write (A7) as

$$\begin{aligned}\frac{\mathrm{d}V}{\mathrm{d}t}=&-\frac{\beta}{2Re}\left(\|\nabla\boldsymbol{v}\|^2+\|\nabla\boldsymbol{u}\|^2\right)-\frac{\alpha(1-\beta)}{2ReWi^2}\,\|\boldsymbol{d}\|^2_{\alpha\boldsymbol{d}}-\langle \boldsymbol{v},\,\boldsymbol{v}\cdot\nabla\boldsymbol{b}\rangle+\frac{1-\beta}{ReWi}\,\langle \boldsymbol{v},\,\nabla\cdot\boldsymbol{c}_b\rangle\\&+\frac{\alpha(1-\beta)}{ReWi}\,\langle \boldsymbol{d}(\boldsymbol{I}+\boldsymbol{d}),\,\nabla\boldsymbol{b}\rangle_{\alpha\boldsymbol{d}}-\frac{1-\beta}{ReWi}\left\langle \boldsymbol{d},\,(\boldsymbol{I}-\alpha\boldsymbol{c}_b)\nabla\boldsymbol{v}+\frac{\alpha}{2}(\boldsymbol{v}\cdot\nabla)\boldsymbol{c}_b\right\rangle_{\alpha\boldsymbol{d}}\\&+\frac{\alpha(1-\beta)}{2ReWi}\left\langle \boldsymbol{d},\,-(\boldsymbol{b}\cdot\nabla)\boldsymbol{c}_b+2(\boldsymbol{c}_b-\boldsymbol{I})\nabla\boldsymbol{b}+\frac{1}{Wi}(\boldsymbol{I}-\boldsymbol{c}_b)\right\rangle_{\alpha\boldsymbol{d}}+\frac{\beta}{2Re}\,\|\nabla\boldsymbol{b}\|^2\,,\end{aligned}\tag{A9}$$

where we have chosen to emphasise the deviation of $\boldsymbol{c}_b$ from $\boldsymbol{I}$, which has modified the first terms in both the second and third lines of the above equation, due to the role that this choice plays in the main result of the paper. This completes the proof of the identity (4.11).

Appendix B. Proof of Lemma 2

Proof. Let $\boldsymbol{c}$ be a positive-definite matrix. We first give an upper bound on the off-diagonal entries c_{ij} in terms of the eigenvalues of $\boldsymbol{c}$. For $i\neq j$, let $\boldsymbol{x}_\pm=\boldsymbol{e}_i\pm\boldsymbol{e}_j$. Then $\|\boldsymbol{x}_\pm\|^2=2$ and

$$\boldsymbol{x}_\pm^{\top}\boldsymbol{c}\,\boldsymbol{x}_\pm=c_{ii}+c_{jj}\pm2c_{ij}.\tag{B1}$$

If λ_{min} and λ_{max} are the minimum and maximum eigenvalues of $\boldsymbol{c}$, the standard Rayleigh quotient bounds imply that

$$2\lambda_{min}\leq c_{ii}+c_{jj}\pm2c_{ij}\leq2\lambda_{max}.\tag{B2}$$

Taking the difference of the two inequalities gives

$$(c_{ii}+c_{jj}+2c_{ij})-(c_{ii}+c_{jj}-2c_{ij})=4c_{ij}\leq2\lambda_{max}-2\lambda_{min}.\tag{B3}$$

Hence,

$$\left|c_{ij}\right|\leq\frac{1}{2}\,(\lambda_{max}-\lambda_{min})\,,\qquad i\neq j.\tag{B4}$$

To complete the proof of the lemma, we must show that

$$(\lambda_{max}-\lambda_{min})\leq a\,\mathrm{tr}\left(\boldsymbol{c}+\boldsymbol{c}^{-1}-2\boldsymbol{I}\right)+b\tag{B5}$$

https://doi.org/10.1017/jfm.2026.11731 Published online by Cambridge University Press

for some constants a, b which we aim to identify. To do this, note first that if $\lambda_i > 0$ are the eigenvalues of $\boldsymbol{c}$, then

$$\mathrm{tr}(\boldsymbol{c}+\boldsymbol{c}^{-1}-2\boldsymbol{I}) = \sum_{i=1}^{3}(\lambda_i+\lambda_i^{-1}-2) \geq (\lambda_{max}+\lambda_{max}^{-1}-2)+(\lambda_{min}+\lambda_{min}^{-1}-2). \quad \text{(B6)}$$

It follows that if a is such that the function

$$F_a(x,y) = y-x-a\left(x+\frac{1}{x}+y+\frac{1}{y}-4\right) \quad \text{(B7)}$$

is bounded above for any $y \geq x > 0$, then (B5) holds with $b = \max_{y\geq x>0} F_a(x,y)$. Elementary calculus shows that F_a is bounded above whenever $a \geq 1$ and, furthermore, that the corresponding maxima are

$$\begin{aligned} b = F_a\left(\sqrt{\frac{a}{a+1}}, \sqrt{\frac{a}{a-1}}\right) &= 4a-2\sqrt{a(a+1)}-2\sqrt{a(a-1)} \\ &= \frac{4}{a(1+\sqrt{1+a^{-1}})(1+\sqrt{1-a^{-1}})(\sqrt{1+a^{-1}}+\sqrt{1-a^{-1}})} \\ &\leq \frac{2\left(2-\sqrt{2}\right)}{a}. \end{aligned} \quad \text{(B8)}$$

The final inequality follows since $a \mapsto (1+\sqrt{1+a^{-1}})(1+\sqrt{1-a^{-1}})(\sqrt{1+a^{-1}}+\sqrt{1-a^{-1}})$ is monotone increasing for $a \geq 1$. To complete the proof, we combine (B4) and (B5) with the above expression and estimate for b to give

$$|c_{ij}| \leq \frac{a}{2}\mathrm{tr}\left(\boldsymbol{c}+\boldsymbol{c}^{-1}-2\boldsymbol{I}\right)+\frac{2-\sqrt{2}}{a}, \quad \text{(B9)}$$

for any $a \geq 1$. □

Appendix C. Proof of Theorem 1

To apply Lemma 1 we must first check that ΛV is bounded along trajectories of the system (2.5*a*–*c*). An analogous argument to that made immediately preceding Theorem 1 shows that, if $\Lambda = 2/(1-Wi)$, then for any $\delta < 4\sqrt{2}\beta/Re$ and any $1 \leq a < 2\delta(1-1/\Lambda)/Wi$ the estimate

$$\Lambda\frac{\mathrm{d}V}{\mathrm{d}t} \leq -c_1\left(\|\nabla \boldsymbol{v}\|^2+\|\boldsymbol{d}\|_{\boldsymbol{d}}^2\right)+c_2 \quad \text{(C1)}$$

holds for some positive constants c_1, c_2 (i.e. δ and a are chosen so as not to quite absorb all the dissipative terms). It then follows from (4.3) that

$$\frac{\mathrm{d}V}{\mathrm{d}t} \leq -cV+\gamma \quad \text{(C2)}$$

for some $c, \gamma > 0$ along trajectories of the system, and we can conclude from Grönwall's lemma that V is bounded along trajectories. Since (4.28) holds, condition (ii) of Lemma 1 holds with

$$\kappa = \frac{\Lambda\beta}{4\delta Re}+(2-\sqrt{2})\frac{\Lambda(1-\beta)}{a\,Re\,Wi}, \quad \text{(C3)}$$

https://doi.org/10.1017/jfm.2026.11731 Published online by Cambridge University Press

and the final bound is computed by substituting the choices (4.29) into the above equation. This completes the proof of Theorem 1.

Appendix D. Proof of Theorem 2

Proof. It is shown in (Binns & Wynn 2024) that, if

$$\alpha = (1 - Wi)\left(1 - \frac{Wi}{\sqrt{1 + Wi^2}}\right), \tag{D1}$$

then $\boldsymbol{I} + \alpha \boldsymbol{d} \succeq \boldsymbol{I} - \alpha \boldsymbol{c}_{steady} \succ 0$.

If $\boldsymbol{c}$ is bounded along trajectories of the system, we have that

$$\overline{\frac{\mathrm{d}}{\mathrm{d}t}\int_\Omega \log\det \boldsymbol{c}\,\mathrm{d}V} = \frac{1}{Wi}\overline{\int_\Omega \mathrm{tr}\left(\boldsymbol{c}^{-1} - \boldsymbol{I}\right)\,\mathrm{d}V} = 0. \tag{D2}$$

This motivates studying the quantity

$$\tilde{\mathcal{E}} = \frac{\beta}{Re}\left\|\nabla \boldsymbol{u}\right\|^2 + \frac{1-\beta}{2Re\,Wi^2}\int_\Omega \mathrm{tr}(\boldsymbol{c} - \boldsymbol{I})\,\mathrm{d}V \tag{D3}$$

since its time average is equal to the time-averaged dissipation rate of the overall system $\overline{\mathcal{E}}$. We now use the fact that $\|\nabla \boldsymbol{u}\|^2 = \|\nabla \boldsymbol{v}\|^2 + \|\nabla \boldsymbol{b}\|^2$ (since $\boldsymbol{b} = \boldsymbol{b}_{steady}$) to decompose $\tilde{\mathcal{E}}$ as

$$\begin{aligned}\tilde{\mathcal{E}} &= \frac{\beta}{Re}\left\|\nabla \boldsymbol{b}\right\|^2 + \frac{1-\beta}{2Re\,Wi^2}\int_\Omega \mathrm{tr}(\boldsymbol{c}_b - \boldsymbol{I})\,\mathrm{d}V + \underbrace{\frac{\beta}{Re}\left\|\nabla \boldsymbol{v}\right\|_2^2 + \frac{1-\beta}{2Re\,Wi^2}\int_\Omega \mathrm{tr}(\boldsymbol{d})\,\mathrm{d}V}_{\mathcal{E}_2} \\ &= \frac{1}{Re} + \mathcal{E}_2.\end{aligned} \tag{D4}$$

We now aim to control $\mathcal{E}_2$ using an appropriately chosen auxiliary functional V whose derivative is given by (4.11). It was shown in (Binns & Wynn 2024) that within the region

$$\frac{\mathrm{tr}(\boldsymbol{I} - \alpha \boldsymbol{c}_b)}{\alpha Wi}\left(\frac{1-\beta}{1-Wi}\right)Wi + \frac{Re}{Re_E} < \beta, \tag{D5}$$

if V is defined with $\boldsymbol{b} = \boldsymbol{b}_{steady}$ and $\boldsymbol{c}_b = \boldsymbol{c}_{steady}$ given by (4.7), then

$$\frac{\mathrm{d}V}{\mathrm{d}t} \le -\varepsilon_1 \left\|\alpha \boldsymbol{d}\right\|_{\alpha \boldsymbol{d}}^2 - \varepsilon_2 \left\|\nabla \boldsymbol{v}\right\|_2^2, \tag{D6}$$

for some constants $\varepsilon_1, \varepsilon_2 > 0$ which depend on the system parameters. This also shows that $\boldsymbol{d}$ and $\boldsymbol{c}$ are bounded along trajectories of the system, whenever (D5) holds. Using (D6) gives

$$\mathcal{E}_2 + \Lambda\frac{\mathrm{d}V}{\mathrm{d}t} \le \left(\frac{\beta}{Re} - \Lambda\epsilon_2\right)\left\|\nabla \boldsymbol{v}\right\|_2^2 + \frac{1-\beta}{2\alpha Re\,Wi^2}\int_\Omega \mathrm{tr}(\alpha \boldsymbol{d})\,\mathrm{d}V - \Lambda\varepsilon_1\left\|\alpha \boldsymbol{d}\right\|_{\alpha \boldsymbol{d}}^2, \tag{D7}$$

https://doi.org/10.1017/jfm.2026.11731 Published online by Cambridge University Press

where we are free to pick the constant Λ. Writing $\gamma = 2\alpha Re\, Wi^2 \Lambda\epsilon_1/(1-\beta)$ and using the identity $\|\boldsymbol{A}-\boldsymbol{I}\|^2_{\boldsymbol{A}-\boldsymbol{I}} = \int_\Omega \mathrm{tr}\big(\boldsymbol{A}+\boldsymbol{A}^{-1}-2\boldsymbol{I}\big)\,\mathrm{d}V$, we have

$$\mathcal{E}_2 + \Lambda\frac{\mathrm{d}V}{\mathrm{d}t} \le \left(\frac{\beta}{Re} - \Lambda\epsilon_2\right)\|\nabla \boldsymbol{v}\|_2^2 \tag{D8}$$

$$+ \frac{1-\beta}{2\alpha Re\, Wi^2}\int_\Omega \mathrm{tr}(\boldsymbol{I}+\alpha\boldsymbol{d}) - \mathrm{tr}\boldsymbol{I} - \gamma\,\mathrm{tr}\left[(\boldsymbol{I}+\alpha\boldsymbol{d})^{-1} + (\boldsymbol{I}+\alpha\boldsymbol{d}) - 2\boldsymbol{I}\right]\mathrm{d}V \tag{D9}$$

$$= \left(\frac{\beta}{Re} - \Lambda\epsilon_2\right)\|\nabla \boldsymbol{v}\|_2^2 + \frac{1-\beta}{2\alpha Re\, Wi^2}\sum_{i=1}^{3}\int_\Omega f_\gamma(\lambda_i)\mathrm{d}V \tag{D10}$$

where $\lambda_i > 0$ are the (necessarily positive) eigenvalues of $\boldsymbol{I}+\alpha\boldsymbol{d}$ and f_γ is the function

$$f_\gamma(x) = x - 1 - \gamma(x + x^{-1} - 2), \qquad x > 0. \tag{D11}$$

If $\gamma > 1$, elementary calculus implies that f_γ has a maximum at $x = \sqrt{\gamma/(\gamma-1)}$ with maximum value

$$\max_{x>0} f_\gamma(x) = 2\gamma - 1 - 2\sqrt{\gamma(\gamma-1)} = \frac{1}{2\gamma - 1 + 2\sqrt{\gamma(\gamma-1)}} \le \frac{1}{\gamma}. \tag{D12}$$

Using this inequality in (D10) gives

$$\mathcal{E}_2 + \Lambda\frac{\mathrm{d}V}{\mathrm{d}t} \le \left(\frac{\beta}{Re} - \Lambda\epsilon_2\right)\|\nabla \boldsymbol{v}\|_2^2 + \frac{3(1-\beta)}{2\alpha Re\, Wi^2\gamma}$$

$$= \left(\frac{\beta}{Re} - \Lambda\epsilon_2\right)\|\nabla \boldsymbol{v}\|_2^2 + \frac{3}{\Lambda\epsilon_1}\left(\frac{(1-\beta)}{2\alpha Re\, Wi^2}\right)^2. \tag{D13}$$

Consequently, if Λ is sufficiently large then there is a constant $c > 0$, independent of Λ for which

$$\mathcal{E}_2 + \Lambda\frac{\mathrm{d}V}{\mathrm{d}t} \le \frac{c}{\Lambda}. \tag{D14}$$

Substituting this expression into (D4) gives

$$\tilde{\mathcal{E}} + \Lambda\frac{\mathrm{d}V}{\mathrm{d}t} \le \frac{1}{Re} + \frac{c}{\Lambda}. \tag{D15}$$

Taking the time average of this expression, and using the fact $\overline{\mathcal{E}} = \overline{\tilde{\mathcal{E}}}$, gives the required bound. □

Appendix E. Proof of (5.4)

Proof. We first write $\boldsymbol{c}$ in terms of its principal leading submatrix $\boldsymbol{c}_{2\times2}$

$$\boldsymbol{c} = \begin{bmatrix} \boldsymbol{c}_{2\times2} & \boldsymbol{m} \\ \boldsymbol{m}^\top & c_{zz} \end{bmatrix}, \qquad \boldsymbol{m} = \begin{bmatrix} c_{xz} \\ c_{yz} \end{bmatrix}, \qquad \boldsymbol{c}_{2\times2} = \begin{bmatrix} c_{xx} & c_{xy} \\ c_{xy} & 1 \end{bmatrix}. \tag{E1}$$

With no-penetration and no-slip boundary conditions in the $\boldsymbol{e}_y$ direction, we consider the streamwise shear component

$$S = \left.\frac{\partial u_x}{\partial y}\right|_{wall} \tag{E2}$$

https://doi.org/10.1017/jfm.2026.11731 Published online by Cambridge University Press

and the governing equations for the components of $\boldsymbol{c}_{2\times2}$ at the walls

$$\frac{\partial c_{xx}}{\partial t} = 2S\, c_{xy} + \frac{1 - c_{xx}}{Wi}, \qquad \frac{\partial c_{xy}}{\partial t} = S\, c_{yy} - \frac{c_{xy}}{Wi}, \qquad \frac{\partial c_{yy}}{\partial t} = \frac{1 - c_{yy}}{Wi}. \tag{E3}$$

Hence,

$$c_{yy}(t) = 1 + \big(c_{yy}(0) - 1\big)\, e^{-t/Wi} \to 1, \qquad \text{as } t \to \infty. \tag{E4}$$

We now assume $c_{yy} = 1$ initially, so that it remains so for all subsequent times. We now analyse the behaviour of the leading principal submatrix at the walls and define its determinant as

$$\Delta = c_{xx} - c_{xy}^2. \tag{E5}$$

The time derivative of the determinant is given by

$$\dot{\Delta} = \frac{\partial c_{xx}}{\partial t} - 2c_{xy}\frac{\partial c_{xy}}{\partial t} = -\frac{c_{xx} - 1}{Wi} + \frac{2c_{xy}^2}{Wi} = \frac{1}{Wi}\left(1 + c_{xy}^2 - \Delta\right), \tag{E6}$$

which gives the equality

$$c_{xy}^2 = (\Delta - 1) + Wi\,\dot{\Delta}. \tag{E7}$$

By utilising the above equalities we obtain

$$\begin{aligned}
\operatorname{tr}\left(\boldsymbol{c}_{2\times2} + \boldsymbol{c}_{2\times2}^{-1} - 2\boldsymbol{I}_{2\times2}\right)\Big|_{wall} &= c_{xx} - 3 + \frac{1 + c_{xx}}{\Delta} \\
&= \left(\Delta + c_{xy}^2 - 3\right) + \frac{1 + \Delta + c_{xy}^2}{\Delta} \\
&= \left(\Delta + \frac{1}{\Delta} - 2\right) + c_{xy}^2\left(1 + \frac{1}{\Delta}\right) \\
&= \left(\Delta + \frac{1}{\Delta} - 2\right) + \left[(\Delta - 1) + Wi\,\dot{\Delta}\right]\left(1 + \frac{1}{\Delta}\right) \\
&= 2(\Delta - 1) + Wi\left(\dot{\Delta} + \frac{\dot{\Delta}}{\Delta}\right).
\end{aligned} \tag{E8}$$

By noticing that

$$\dot{\Delta} + \frac{\dot{\Delta}}{\Delta} = \frac{\mathrm{d}}{\mathrm{d}t}\left(\Delta + \log\Delta\right) \tag{E9}$$

and utilising the property of infinite-time averages

$$\overline{\operatorname{tr}\left(\boldsymbol{c}_{2\times2} + \boldsymbol{c}_{2\times2}^{-1} - 2\boldsymbol{I}_{2\times2}\right)\Big|_{wall}} = 2\left(\overline{\Delta} - 1\right) + Wi\,\overline{\frac{\mathrm{d}}{\mathrm{d}t}\left(\Delta + \log\Delta\right)} = 2\left(\overline{\Delta} - 1\right). \tag{E10}$$

Similarly, we find

$$\overline{c_{xy}^2} = \overline{\Delta} - 1 + Wi\,\overline{\dot{\Delta}} = \overline{\Delta} - 1, \tag{E11}$$

which leads to

$$2\overline{c_{xy}^2} = \overline{\operatorname{tr}\left(\boldsymbol{c}_{2\times2} + \boldsymbol{c}_{2\times2}^{-1} - 2\boldsymbol{I}_{2\times2}\right)\Big|_{wall}}. \tag{E12}$$

The final step then involves proving

$$\overline{\operatorname{tr}\left(\boldsymbol{c}_{2\times2} + \boldsymbol{c}_{2\times2}^{-1} - 2\boldsymbol{I}_{2\times2}\right)\Big|_{wall}} \le \overline{\operatorname{tr}\left(\boldsymbol{c} + \boldsymbol{c}^{-1} - 2\boldsymbol{I}\right)\Big|_{wall}}. \tag{E13}$$

https://doi.org/10.1017/jfm.2026.11731 Published online by Cambridge University Press

We consider the decomposition

$$\operatorname{tr}\left(\boldsymbol{c}+\boldsymbol{c}^{-1}-2\boldsymbol{I}\right)=\operatorname{tr}\left(\boldsymbol{c}_{2\times2}+\left(\boldsymbol{c}^{-1}\right)_{2\times2}-2\boldsymbol{I}_{2\times2}\right)+\left[c_{zz}+\left(\boldsymbol{c}^{-1}\right)_{zz}-2\right]. \tag{E14}$$

For a positive-definite matrix $\boldsymbol{c}$, the properties of Schur complements (Horn & Johnson 2013, Theorem 7.7.15) imply that

$$\left(\boldsymbol{c}^{-1}\right)_{2\times2}\succeq\boldsymbol{c}_{2\times2}^{-1}, \tag{E15}$$

and thus

$$\operatorname{tr}\left[\left(\boldsymbol{c}^{-1}\right)_{2\times2}\right]\geq\operatorname{tr}\left(\boldsymbol{c}_{2\times2}^{-1}\right). \tag{E16}$$

Similarly we find

$$\left(\boldsymbol{c}^{-1}\right)_{zz}\geq\frac{1}{c_{zz}}. \tag{E17}$$

Hence, from the above estimates and (E14) we have

$$\begin{aligned}\operatorname{tr}\left(\boldsymbol{c}+\boldsymbol{c}^{-1}-2\boldsymbol{I}\right)&\geq\operatorname{tr}\left(\boldsymbol{c}_{2\times2}+\boldsymbol{c}_{2\times2}^{-1}-2\boldsymbol{I}_{2\times2}\right)+\left(c_{zz}+\frac{1}{c_{zz}}-2\right)\\&\geq\operatorname{tr}\left(\boldsymbol{c}_{2\times2}+\boldsymbol{c}_{2\times2}^{-1}-2\boldsymbol{I}_{2\times2}\right).\end{aligned} \tag{E18}$$

Combining the above inequality with (E12) gives

$$2\overline{c_{xy}^2}\leq\overline{\operatorname{tr}\left(\boldsymbol{c}+\boldsymbol{c}^{-1}-2\boldsymbol{I}\right)\big|_{wall}}, \tag{E19}$$

as desired. □

References

Balci, N., Thomases, B., Renardy, M. & Doering, C.D. 2011 Symmetric factorization of the conformation tensor in viscoelastic fluid models. *J. Non-Newtonian Fluid Mech.* **166**, 546–553.

Binns, J. & Wynn, A. 2024 Global stability of Oldroyd-B fluids in plane Couette flow. *J. Non-Newtonian Fluid Mech.* **324**, 105171.

Boyaval, S., Lelièvre, T. & Mangoubi, C. 2009 Free-energy-dissipative schemes for the Oldroyd-B model. *ESAIM: Modélisation Math. Anal. Numérique* **43**, 523–561.

Busse, F.H. 1978 Non-linear properties of thermal convection. *Rep. Prog. Phys.* **41** (12), 1929–1967.

Chernyshenko, S.I. 2022 Relationship between the methods of bounding time averages. *Phil. Trans. R. Soc. Lond. A* **380** (2225), 20210044.

Chernyshenko, S.I., Goulart, P., Huang, D. & Papachristodoulou, A. 2014 Polynomial sum of squares in fluid dynamics: a review with a look ahead. *Phil. Trans. R. Soc. Lond. A* **372**, 20130350.

Doering, C.R. & Constantin, P. 1992 Energy dissipation in shear driven turbulence. *Phys. Rev. Lett.* **69**, 1648–1651.

Doering, C.R. & Constantin, P. 1994 Variational bounds on energy dissipation in incompressible flows: shear flow. *Phys. Rev. E* **49**, 4087–4099.

Doering, C.R. & Constantin, P. 1995 Variational bounds on energy dissipation in incompressible flows. II. Channel flow. *Phys. Rev. E* **51**, 3192–3198.

Doering, C.R., Eckhardt, B. & Schumacher, J. 2006 Failure of energy stability in Oldroyd-B fluids at arbitrarily low Reynolds numbers. *J. Non-Newtonian Fluid Mech.* **135**, 92–96.

Groisman, A. & Steinberg, V. 1996 Couette–Taylor flow in a dilute polymer solution. *Phys. Rev. Lett.* **77**, 1480–1483.

Groisman, A. & Steinberg, V. 1998 Mechanism of elastic instability in Couette flow of polymer solutions: experiment. *Phys. Fluids* **10**, 2451–2463.

Groisman, A. & Steinberg, V. 2000 Elastic turbulence in a polymer solution flow. *Nature* **405**, 53–55.

https://doi.org/10.1017/jfm.2026.11731 Published online by Cambridge University Press

HOPF, E. 1950 Über die anfangswertaufgabe für die hydrodynamischen grundgleichungen. *Math. Nachr.* **4**, 213–231.
HORN, R.A. & JOHNSON, C.R. 2013 *Matrix Analysis*, 2nd edn. Cambridge University Press.
HOWARD, L.N. 1963 Heat transport by turbulent convection. *J. Fluid Mech.* **17**, 405–432.
HU, D. & LELIÈVRE, T. 2007 New entropy estimates for the Oldroyd-B model, and related models. *Commun. Math. Sci.* **5** (4), 909–916.
JONES, W.M. & MADDOCK, J.L. 1966 Onset of instabilities and reduction of drag in the flow of relaxing liquids through tubes and porous beds. *Nature* **212**, 388–390.
KEILLER, R.A. 1992 Numerical instability of time-dependent flows. *J. Non-Newtonian Fluid Mech.* **43**, 229–246.
KEUNINGS, R. 1986 On the high Weissenberg number problem. *J. Non-Newtonian Fluid Mech.* **20**, 209–226.
LARSON, R.G., SHAQFEH, E.S.G. & MULLER, S.J. 1990 A purely elastic instability in Taylor–Couette flow. *J. Fluid Mech.* **218**, 573–600.
LEE, J., HWANG, W. & CHO, K. 2021 Effect of stress diffusion on the Oldroyd-B fluid flow past a confined cylinder. *J. Non-Newtonian Fluid Mech.* **297**, 104650.
LOZINSKI, A. & OWENS, R.G. 2003 An energy estimate for the Oldroyd-B model: theory and applications. *J. Non-Newtonian Fluid Mech.* **112**, 161–176.
LUKÁČOVÁ−MEDVID'OVÁ, M., NOTSU, H. & SHE, B. 2016 Energy dissipative characteristic schemes for the diffusive Oldroyd-B viscoelastic fluid. *Intl J. Numer. Meth. Fluids* **81** (9), 523–557.
METZNER, A.B. & PARK, M.G. 1964 Turbulent flow characteristics of viscoelastic fluids. *J. Fluid Mech.* **20**, 291–303.
METZNER, A.B. & WHITE, J.L. 1965 Flow behavior of viscoelastic fluids in the inlet region of a channel. *AIChE J.* **11**, 989–995.
NICODEMUS, R., GROSSMANN, S. & HOLTHAUS, M. 1997*a* Improved variational principle for bounds on energy dissipation in turbulent shear flow. *Physica D* **101**, 178–190.
NICODEMUS, R., GROSSMANN, S. & HOLTHAUS, M. 1997*b* Variational bound on energy dissipation in plane Couette flow. *Phys. Rev. E* **56**, 6774–6786.
NICODEMUS, R., GROSSMANN, S. & HOLTHAUS, M. 1998 The background flow method. Part 1. Constructive approach to bounds on energy dissipation. *J. Fluid Mech.* **363**, 281–300.
PLASTING, S.C. & KERSWELL, R.R. 2003 Improved upper bound on the energy dissipation rate in plane Couette flow: the full solution to Busse's problem and the Constantin–Doering–Hopf problem with one-dimensional background field. *J. Fluid Mech.* **477**, 363–379.
RAJKOTIA-ZAHEER, F. & GOLUSKIN, D. 2026 Bounds on dissipation in three-dimensional planar shear flows: reduction to two-dimensional problems. *J. Fluid Mech.* **1026**, A8.
RENARDY, M. 1992 A rigorous stability proof for plane Couette flow of an upper convected Maxwell fluid at zero Reynolds number. *Eur. J. Mech. B Fluids* **11** (4), 511–516.
RENARDY, M. 1993 On the stability of parallel shear flow of an Oldroyd B fluid. *Differ. Integral Equ.* **6** (3), 481–489.
RENARDY, M. & THOMASES, B. 2021 A mathematician's perspective on the Oldroyd-B model: progress and future challenges. *J. Non-Newtonian Fluid Mech.* **293**, 104573.
ROSA, R. & TEMAM, R.M. 2020 Optimal minimax bounds for time and ensemble averages for the incompressible Navier–Stokes equations. arXiv preprint arXiv: 2010.06730.
ROTHSTEIN, J.P. & MCKINLEY, G.H. 2001 The axisymmetric contraction–expansion: the role of extensional rheology on vortex growth dynamics and the enhanced pressure drop. *J. Non-Newtonian Fluid Mech.* **98**, 33–63.
SAMANTA, D., DUBIEF, Y., HOLZNER, M., SCHÄFER, C., MOROZOV, A.N., WAGNER, C. & HOF, B. 2013 Elasto-inertial turbulence. *Proc. Natl Acad. Sci. USA* **110** (26), 10557–10562.
SHAQFEH, E.S.G. 1996 Purely elastic instabilities in viscometric flows. *Annu. Rev. Fluid Mech.* **28**, 129–185.
THOMASES, B. & SHELLEY, M. 2007 Emergence of singular structures in Oldroyd-B fluids. *Phys. Fluids* **19**, 103103.
TOBASCO, I., GOLUSKIN, D. & DOERING, C.R. 2018 Optimal bounds and extremal trajectories for time averages in nonlinear dynamical systems. *Phys. Lett. A* **382** (6), 382–386.
VIRK, P.S. 1975 Drag reduction fundamentals. *AIChE J.* **21** (4), 625–656.

https://doi.org/10.1017/jfm.2026.11731 Published online by Cambridge University Press